Impacts of climate and reclamation on temporal variations in CH_4 emissions from different wetlands in China: From 1950 to 2010

Running title: CH_4 from Chinese natural wetlands

Tingting Li[1], Wen Zhang[1,*], Qing Zhang[1], Yanyu Lu[2], Guocheng Wang[1], Zhenguo Niu[3], Maarit Raivonen[4], Timo Vesala[4,5]

[1] LAPC, Institute of Atmospheric Physics, Chinese Academy of Sciences, Beijing, 100029, China

[2] Anhui Climate Center, Hefei, 230031, China

[3] State Key Laboratory of Remote Sensing Science, Jointly Sponsored by Institute of Remote Sensing Applications, Chinese Academy of Sciences and Beijing Normal University, Beijing 100101, China;

[4] Department of Physics, P.O. Box 48, FI-00014 University of Helsinki, Finland

[5] Department of Forest Sciences, P.O. Box 27, FI-00014 University of Helsinki, Finland

Correspondence to: Wen Zhang (Email: zhw@mail.iap.ac.cn, Tel: 86-10-62071389)

Keywords: CH_4 emissions, wetland, modeling, temporal variation, China

Abstract

Natural wetlands are among the most important sources of methane; thus, these areas are important for better understanding long-term temporal variations in atmospheric methane concentration. During the last 60 years, wetlands have experienced extensive conversion and global impacts from climate warming, which makes the estimation of methane emission from wetlands highly uncertain. In this paper, we present a modeling framework, integrating $CH4MOD_{wetland}$, TOPMODEL and TEM models, to analyze the temporal and spatial variations in CH_4 emissions from natural wetlands (including inland wetlands, coastal wetlands, lakes and rivers) in China. Our analysis revealed an increase of 25.5%, averaging 0.52 g m^{-2} per decade, in national CH_4 fluxes from 1950 to 2010, which was mainly induced by climate warming. Higher rates of increasing CH_4 fluxes occurred in northeastern, northern and northwestern China, associated with large temperature increases. However, decreases in precipitation due to climate warming offset the increase in CH_4 fluxes in these regions. The CH_4 fluxes from the wetland on the Qinghai Tibetan Plateau exhibited a lower rate of increase, which was approximately 25% of that simulated in northeastern China. Although climate warming has accelerated CH_4 fluxes, the total

amount of national CH_4 emissions decreased by approximately 2.35 Tg (1.91－2.81 Tg), i.e., from 4.50 Tg in the early 1950s to 2.15 Tg in the late 2000s, due to a large wetland loss of 17.0 million ha. Of this reduction, 0.26 Tg (0.24－0.28 Tg) was derived from lakes and rivers, 0.16 Tg (0.13－0.20 Tg) from coastal wetlands, and 1.92 Tg (1.54－2.33 Tg) from inland wetlands. Northeastern China had the largest contribution to this reduction, with a loss of 1.68 Tg. The CH_4 emissions were reduced by more than half in most regions in China except for the Qinghai Tibetan Plateau, where only a 23.3% decrease in CH_4 was observed.

1. Introduction

Atmospheric methane (CH_4) is the second most important trace greenhouse gas (GHG) after carbon dioxide (CO_2). The direct radiative forcing for CH_4 is 50 times greater than that of CO_2 over a 100-year period (IPCC, 2013). In the atmosphere, the direct radiative forcing of CH_4 was calculated to be 0.48 W m^{-2} by IPCC (2007); this value was revised to 0.97 W m^{-2} when its indirect global warming effect was incorporated (IPCC, 2013; Forster et al., 2007; Shindell et al., 2009). In 2011, the concentration of atmospheric CH_4 reached 1803.2 ppb, which was 150% greater than before 1750 (IPCC, 2013). However, unlike the rigid temporal increase of atmospheric CO_2, atmospheric CH_4 has exhibited remarkable temporal variations in conjunction with a long-term increasing trend, remaining nearly constant from 1999 to 2006, then continuing to increase after 2007 (Nisbet et al., 2014).

While the majority of CH_4 sinks remain relatively stable, variations in atmospheric CH_4 have been attributed to CH_4 sources. Among the global CH_4 emission sources, natural wetlands are one of the most important contributors (Denman et al., 2007; Potter et al., 2006; Whalen, 2005). The methane emissions from wetlands account for 20－25% of the global annual atmospheric emissions, although the uncertainties are relatively large (IPCC, 2007; Mitsch and Gosselink, 2007). During the 20th century, half of the world's wetlands were lost (Moser et al., 1996; Revenga et al., 2000). In China, natural wetlands have also experienced a serious loss during the past 60 years, attributed primarily to cropland reclamation (An et al., 2007; Niu et al., 2012; Huang et al., 2010; Xu and Tian, 2012). Based on remote sensing data, Niu et al. (2012) reported that approximately 33% of the wetlands were lost between 1978 and 2008. An et al. (2007) estimated that 23% of freshwater swamps,

16% of lakes, 15% of rivers, and 51% of coastal wetlands were lost between 1950 and 2000 based on census data.

Multiple studies for estimating CH_4 emissions in China have been conducted; most of these works have involved the extrapolation of site-specific measurements to the region (Wang et al., 1993; Khail et al., 1993; Jin et al., 1999; Ding et al., 2004; 2007; Chen et al., 2013; Wang et al., 2012). However, substantial spatial and seasonal variations in CH_4 emissions from natural wetlands are often observed (e.g., Christensen et al., 2003; Ding et al., 2004; Yang et al., 2006) because of the complex physiological processes of plants and microorganisms, which are regulated by climatic and edaphic factors (Cao et al., 1998).

Some modelers have simulated national CH_4 emissions from marshlands for the last 60 years (e.g., Xu and Tian, 2012; Tian et al., 2011) based on census data collected in areas that were historically wetlands. To date, there has been no comprehensive study on national, long-term CH_4 emissions from all natural wetlands, including freshwater marshes, coastal wetlands, lakes and rivers in China.

A remote sensing study presented a comprehensive map of the change in natural wetlands that occurred between 1978 and 2008 in China (Niu et al., 2012). The objectives of the present study are to analyze the spatial and temporal changes in CH_4 emissions across China's natural wetlands to quantify the impact of climate change and anthropogenic activities on CH_4 emissions from the natural wetlands in different regions of China.

2. Materials and Methods

In this research, the primary natural wetland types include coastal wetlands, lakes and rivers, and other types that are defined as inland wetlands (e.g., marshes, peatlands, and floodplains). In the present study, we used a modified biogeophysical model, called $CH4MOD_{wetland}$ (Li et al., 2010), to simulate CH_4 emissions from inland wetlands and coastal wetlands. Because $CH4MOD_{wetland}$ is not capable of simulating CH_4 emissions from lakes and rivers, we directly extrapolated site-level field measurements (see Supplementary material S1) to estimate the CH_4 emissions from lakes and rivers (Chen et al., 2013).

2.1 Model framework

Fig. 1 shows the model framework for this study. Three models were used with a spatial resolution of 0.5 ° for the period from 1950 to 2010. The main model was a

process-based biogeophysical model, i.e., $CH4MOD_{wetland}$ (Li et al., 2010). $CH4MOD_{wetland}$ is a biogeophysical model that aims to simulate CH_4 production, oxidation and emissions from natural wetlands (Li et al., 2010). This model adopts the hypothesis of the CH4MOD model (Huang et al., 1998, 2004, 2006; Zhang et al., 2011), which is used to simulate CH_4 production, oxidation and emissions from rice paddies. Based on the different sources of methanogenic substrates between natural wetlands and rice paddies, modifications were made so that the model would fit natural wetlands. In $CH4MOD_{wetland}$, methane production rates are determined using the availability of methanogenic substrates and the influences of environmental factors. In $CH4MOD_{wetland}$, the methanogenic substrates are derived from root exudation and the decomposition of above- and below-ground plant litter and soil organic matter. Plant-mediated transport is a primary mechanism of CH_4 emissions, and CH_4 emissions via ebullition are significant in the early stages of plant growth.

The model inputs include daily soil temperature, water table depth, annual aboveground net primary productivity (*ANPP*) and soil texture. The outputs include daily and annual CH_4 production and emissions. Using $CH4MOD_{wetland}$, it is possible to simulate CH_4 emissions from several types of natural wetlands because $CH4MOD_{wetland}$ was validated against independent field measurements of CH_4 flux from different wetland sites across China, Canada and the USA (Li et al., 2010). More details regarding $CH4MOD_{wetland}$ have been documented in previous studies (Li et al., 2010; 2012).

In $CH4MOD_{wetland}$, the environmental factors that influence CH_4 production and emissions in natural wetlands include soil temperature, soil texture and soil redox potential. This model simulated CH_4 fluxes by using inputs of soil texture (soil sand fraction, soil organic carbon and bulk density), aboveground net primary productivity (*ANPP*), daily soil temperature, water table depth and salinity. Then, we multiplied the CH_4 fluxes by the wetland area in each grid and summed the CH_4 emissions from all grids to calculate the total national CH_4 emissions. To make the model useful for coastal wetlands, some modifications were made in this study. For details concerning the modifications made to $CH4MOD_{wetland}$, please see Supplementary material S2.

To obtain regional datasets of ANPP, soil temperature and water table depth for use at a national scale, we used the outputs of the Terrestrial Ecosystem Model (TEM) (Melillo et al., 1993; Zhuang et al., 2004; 2006; 2007; 2013) and the TOPMODEL (Beven and Kirby, 1979) to drive $CH4MOD_{wetland}$.

The TEM model is also a process-based biogeochemistry model that couples carbon, nitrogen, water, and heat processes in terrestrial ecosystems to simulate ecosystem carbon and nitrogen dynamics. This model has been widely used to investigate regional and global NPP (e.g., Melillo et al., 1993; Cramer et al., 1999; McGuire et al., 1992). With this model framework (Fig. 1), the soil temperature and net primary productivity (NPP) outputs from the TEM model were used to drive $CH4MOD_{wetland}$. The fraction of ANPP to NPP was determined based on Gill and Jackson (2003). More descriptions of the model and the inputs are described in Zhuang et al. (2013).

TOPMODEL is a conceptual rainfall-runoff model that is designed to work at the scale of large watersheds using the statistics of topography. In previous research (Bohn et al., 2007; Kleinen et al., 2012; Lu and Zhuang et al., 2012; Zhu et al., 2013), TOPMODEL has been widely used to simulate water table variations in natural wetlands. The TOPMODEL inputs included soil moisture and the topographic wetness index (Fig. 1). The outputs (water table depth) were used to drive $CH4MOD_{wetland}$ (Fig. 1). More details on simulating water table depth using TOPMODL are provided in Supplementary material S2.

2.2 Model calibration

When establishing $CH4MOD_{wetland}$, we used a minimal number of input parameters to allow the use of the model at the regional scale. The model parameters are mainly related to vegetation e.g., the proportion of roots to the total production (f_{root}), the vegetation index (VI), the fraction of CH_4 oxidized during plant-mediated transport (P_{ox}) and the fraction of available plant mediated transport (T_{veg}). f_{root} and T_{veg} were obtained from the literature (please see Table S3 in Supplementary material S2). f_{root} was obtained from Gill and Jackson (2000). According to Walter et al. (2000), shrubs do not contribute to plant mediated transport, trees are poor gas transporters and grasses are good gas transporters. In this study, we defined T_{veg} as 1 for grass and 0 for shrubs and trees, which means that CH_4 can be transported only by ebullition and diffusion in the wetlands containing trees and shrubs. Both VI and P_{ox} are associated with plant species. VI is a vegetation index that can identify the relative differences of methane production among vegetation types, and P_{ox} recognizes different fractions of CH_4 oxidized when transported by different plant species In previous studies, we parameterized VI and P_{ox} using independent CH_4 flux measurements collected from

the Sanjiang Plain (SJ site in Table S2) in region I (Fig. 2), where the dominant plant species is *Carex* (Supplementary material S3) (Li et al., 2010, 2012). In addition, we validated the model at wetland sites using the dominant vegetation type *Carex* in the USA and Canada while *VI* and P_{ox} remained unchanged (Li et al., 2010). In this study, we held *VI* and P_{ox} constant at the sites (REG and HB in Table S2) and across the regions i.e., northeastern China (Region I in Fig. 1), the Qinghai Tibetan Plateau (Region II in Fig. 1) and southern China (Region V in Fig. 1), because these sites and regions are dominated by *Carex* (Supplementary material S3). However, *VI* and P_{ox} should be recalibrated for other wetland sites (Table S2) and regions dominated by *Phragmites* (Region III and IV in Fig. 1). We parameterized *VI* and P_{ox} by minimizing the differences between the observed and simulated fluxes at Wuliangsu Lake in Inner Mongolia (WLS site in Table S2). By setting an increment of 0.1 for *VI* and P_{ox}, the model was run for all combinations of *VI* within the range 0.5－3.0 and P_{ox} within the range 0.1－1 until the root-mean-square error (RMSE) between the daily simulated and observed CH_4 fluxes was minimized. After setting *VI* and P_{ox}, the empirical constant of the salinity influence *a* ([Eqn (S2.1)] in Supplementary material S2) was calibrated by minimizing the root mean-square error (RMSE) between the observed and simulated fluxes at a coastal wetland on Chongming Island in Shanghai Province (CMI site in Table S2). Table S3 (in Supplementary material S2) shows the detailed definition and values of model inputs and parameters.

2.3 Model validation

After model coupling and calibration, model validation is necessary to determine if the model can be used at a national scale. We used independently observed data (different than the data that was used to calibrate the model) to validate the model at the "site-scale" using individual $CH4MOD_{wetland}$ simulations and at the "grid-scale" using the proposed model framework (Fig. 1). More details regarding the "site-scale" and the "grid-scale" validations are described in Supplementary material S2.

The "site-scale" validation showed that the simulated seasonal patterns of daily CH_4 emissions agreed with the observed data at the wetland sites on the Sanjiang Plain (Figure S1a, S1b), the Ruoergai Plateau, (REG in Table S2; Figure S1d, S1e), the Haibei alpine marsh (HB in Table S2; Figure S1g), the Zhalong wetland (ZL in Table S2; Figure S1i) and the Liao River delta (LRD in Table S2; Figure S1k). The regression of simulated versus observed monthly CH_4 fluxes resulted in an R^2 of 0.79,

with a slope of 0.86 and an intercept of 0.73 (n=41, p<0.001) for the "site-scale" validation (Figure S2a). The RMSE, mean deviation (RMD) and the model efficiency (EF) between the simulated and observed monthly CH_4 fluxes were 48.5%, 0.9% and 0.78, respectively.

The "grid-scale" validation showed that the integrated model framework ($CH4MOD_{wetland}$/TEM/TOPMODEL) (Fig. 1) was able to simulate the seasonal variations in monthly CH_4 emissions at the SJ (Figure S1c) and LRD (Figure S1l) sites. Although there are some underestimations in the CH_4 fluxes were predicted by the model framework for the other 3 sites (Figure S1f, S1h and S1j), the measured monthly CH_4 fluxes fell in or near the range of the modeled CH_4 emissions (Figure S2b). For the "grid-scale" validation, the regression of simulated versus observed monthly CH_4 emissions resulted in an R^2 of 0.79, with a slope of 0.84 and an intercept of -0.11 (n=41, p<0.001). The RMSE, RMD and EF between the simulated and observed monthly CH_4 fluxes were 51.3%, -17.8% and 0.75, respectively, for the integrated model framework.

2.4 The extrapolation of the model framework

The extrapolation of this model framework to the national scale (Fig. 1) was based on a wetland division map (Lang and Zu, 1983) (Fig. 2) and a gridded wetland distribution map (Niu et al., 2012) (Fig. 2) of China. Chinese wetlands were divided into five regions according to the location and vegetation type. More details regarding the division of the wetlands are described in Supplementary material S3. For the inland wetlands, we classified the parameters according to the wetland division map. We extrapolated the *VI* and P_{ox} from a wetland site to the region in which it is located. The model parameters at SJ, HB, and WLS (Table S3) were assigned to Region I, Region II and Region III, respectively. In Region IV, we used the parameters for WLS because *Phragmites* is the dominant species in both Region III and Region IV (Table S2). The model parameters for REG (Table S3) were allocated to Region V because this wetland is located at the edge of this region. The coastal wetland parameters were assigned based on LRD and CMI (Table S3).

The gridded wetland distribution maps were presented by Niu et al., (2012) at a resolution of 1 km×1 km. We compiled the data from the gridded wetland maps to generate a dataset of 0.5°×0.5° spatial resolution. We established gridded (0.5°×0.5°), geo-referenced, time-series input datasets of climatic factors (including daily

temperature, precipitation, humidity, and solar radiation) and the soil data (including soil sand percentage, soil bulk density, soil organic carbon and the soil moisture), the water table data and the salinity data for all of China. The climate and soil texture data were used to drive the TEM model (Fig. 1). The soil moisture and topographic wetness index data were used as inputs for TOPMODEL (Fig. 1). Then, $CH4MOD_{wetland}$ was run with the *ANPP*, soil temperature, water table depth, soil texture, and salinity data in each grid cell to estimate the CH_4 fluxes (Fig. 1). The total CH_4 emissions from each grid cell were determined based on the product of the CH_4 fluxes and the wetland area.

2.5 Uncertainty analysis

Uncertainty in the estimated regional CH_4 emissions from natural wetlands may originate from many factors. In this study, we paid more attention to the uncertainties induced by the inputs of ANPP, water table depth and soil sand fraction using the extreme condition approach for uncertainty propagation (Du and Chen, 1999; Li et al., 2012). We set the maximum and minimum values of the input data to be ±10% of the baseline values. Eight simulations were performed to estimate the uncertainties.

2.6 Data sources

We selected seven natural wetlands where extensive field measurements were available for model calibration and model validation. These sites included two marshes, two floodplains, one peatland and two coastal wetlands (Table S2). Fig. 2 shows the locations of the sites. More detailed site descriptions are provided in Table S2.

The gridded wetland maps for 1978, 1990, 2000 and 2008 were obtained from Niu et al. (2012). The method for obtaining the gridded wetland map for 1950 was based on both Niu et al. (2012) and An et al. (2007). An et al. (2007) reported that inland wetland areas lost 23.0%, lake areas lost 16.1%, river areas lost 15.3%, and coastal wetland areas lost 51.2% of their area between 1950 and 2000 in China. To use inland wetlands as an example, we first separated the Sanjiang Plain because more detailed and accurate data could be obtained for that area. Then, we assumed the annual loss rate of inland wetlands was constant between 1950 and 2000. We calculated the annual loss of the inland wetlands between 1950 and 2000 based on An et al. (2007). We regarded this ratio as the annual loss rate of inland wetlands between 1950 and 1978. We also assumed this annual loss rate occurred in every inland

wetland grid cell. The inland wetland area in each grid cell in 1950 was determined using the above annual loss rate as well as the wetland area reported to exist in 1978 based on Niu et al. (2012). Niu et al. (2012) combined floodplains and rivers as river wetlands in his paper; however, because floodplains are always dominated by vascular plants, we included floodplains in the inland wetland category. The fraction of floodplains was based on original satellite data (Z. G. Niu, personal communication, 2013). The wetland area included from the Sanjiang Plain in 1950 was from previous studies (Liu and Ma, 2000; Li et al., 2012; Huang et al., 2010; Ding et al., 2004; 2007). The method used to calculate the lake, river and coastal wetland areas was the same as for the inland wetlands.

Daily climate datasets used for driving the TEM model were developed from the latest monthly air temperature, precipitation, vapor pressure, and cloudiness datasets from the Climatic Research Unit (CRU TS 3.10) of the University of East Anglia in the United Kingdom (Harris et al., 2014).

The soil moisture data were from Fan and van den Dool (2004) (http://www.cpc.ncep.noaa.gov/soilmst/leaky_glb.htm). The soil texture data were derived from the soil map of the Food and Agriculture Organization (FAO, 2012). Soil sand fraction data were used as input to $CH4MOD_{wetland}$, whereas, soil texture data were used to assign the texture-specific parameters to each grid cell in the TEM model (Zhuang et al., 2013). Soil organic carbon content and the reference bulk density in wetland soils were from the Harmonized World Soil Database (HWSD) (FAO, 2008).

The plant phenology and *ANPP* were from the TEM outputs data. The vegetation map of IGBP was referenced to specify vegetation parameters for $CH4MOD_{wetland}$ and TEM. The map was derived from the IGBP Data and Information System (DIS) DISCover Database (Belward et al., 1999; Loveland et al., 2000). The 1 km × 1 km DISCover dataset was reclassified into the TEM vegetation classification scheme and then aggregated to a resolution of 0.5 °×0.5 °.

The topographic wetness index data were from the HYDRO1k Elevation Derivative Database, which was developed by the U.S. Geological Survey Earth Resources Observation and Science (EROS) Center (http://gcmd.nasa.gov/records/GCMD_HYDRO1k.html) (USGS, 2000). The global salinity database was from the World Ocean Atlas 2009 (Antonov et al., 2010).

3. Results

3.1 CH_4 fluxes with changes in climate from 1950 to 2010

The temporal change in CH_4 fluxes (CH_4 emissions per area) were determined based on the climate. In this section, we analyze the climate change-driven seasonal and interannual variations in CH_4 fluxes from the inland wetlands and the coastal wetlands from 1950 to 2010.

Fig. 3 shows the seasonal variations of the modeled average CH_4 fluxes from the 1950s to 2010s. A consistent pattern of peak CH_4 fluxes occurred at the end of July across all regions (Fig. 3). The peak CH_4 fluxes corresponded with the highest NPP and temperature. CH_4 fluxes were very low in January and February, especially in northern China and in the Qinghai Tibetan Plateau (Fig. 3a, b and c), which is consistent with the observed deepest frozen soil. In the warmer regions, such as Region V, CH_4 fluxes were much greater (Fig. 3e). The intra-annual changes of CH_4 fluxes were highest in southern China (Region V), ranging from 6.38－7.37 mg m^{-2} h^{-1} (Fig. 3e), followed by in northeastern China (Region I), ranging from 6.35－7.24 mg m^{-2} h^{-1} (Fig. 3a). The Qinghai Tibetan Plateau (Region II) had the lowest intra-annual change of 1.72－1.98 mg m^{-2} h^{-1} (Fig. 3b). The intra-annual changes were highest in the 2000s in all of the regions. The lowest change occurred in the 1970s in regions I, II, III (Fig. 3a, b and c) and in the 1960s in regions IV, V.

Fig. 4f provides the inter-annual variation and trend in the modeled national annual CH_4 flux in China. The national annual CH_4 flux significantly increased over the last 60 years, especially since the 1980s. The national annual CH_4 flux increased from 16.9 g m^{-2} yr^{-1} in 1950 to 21.2 g m^{-2} yr^{-1} in 2010, a total increase of 26% or an average rate of 0.52 g m^{-2} per decade. The annual CH_4 fluxes fluctuated between 16.0 g m^{-2} yr^{-1} and 19.0 g m^{-2} yr^{-1} before 1980, then increasing rapidly in the 1990s. The highest CH_4 flux, i.e., 22.5 g m^{-2} yr^{-1}, occurred in 1998, whereas the lowest value, 15.7 g m^{-2} yr^{-1}, occurred in 1954.

The estimated annual CH_4 fluxes in different regions are illustrated in Fig. 4a, b, c, d and e. The regions with the largest CH_4 fluxes are northeastern China (Region I, with an average annual mean of 24.8 g m^{-2} yr^{-1}; Fig. 4a) and southern China (Region V, with an average annual mean of 20.1 g m^{-2} yr^{-1}; Fig. 4e). On the Qinghai Tibetan Plateau (Region II), the simulated CH_4 fluxes exhibited the lowest fluxes (Fig. 4b), with an average annual mean of 6.2 g m^{-2} over the same period, which was lower than

Region I by approximately 75% (Fig. 4a). Compared with Region I, the average CH_4 fluxes in Inner Mongolia and northwestern China (Region III) and over the North China Plain and the Middle-Lower Yangtze Plain (Region IV) were lower by 46% to 64% during the past 60 years.

Fig. 4 also provides the trends in the annual CH_4 fluxes in different regions. Except for Region IV (Fig. 4d; $p>0.05$), the annual CH_4 fluxes exhibited significant increases in other regions (Fig. 4a,b,c,d and e; $p<0.001$). The greatest rate of increase in CH_4 fluxes occurred in Region I, i.e., 0.67 g m^{-2} per decade (Fig. 4a), followed by Region V and Region III, i.e., 0.54 g m^{-2} per decade (Fig. 4e) and 0.42 g m^{-2} per decade (Fig. 4c), respectively. In Region IV, the rate of increase in CH_4 fluxes was 0.50 g m^{-2} per decade, although this rate was not significant (Fig. 4d). The smallest rate of increase occurred in Region II (Fig. 4b), i.e., approximately 25% of the rate for Region I (Fig. 4a).

Climate factors can account for the difference in the rates of increase in CH_4 fluxes among the regions noted above. First, a higher temperature will enhance the rate of microbial CH_4 production. Second, an increase in precipitation may result in a higher water table position and promote plant growth, which can accelerate CH_4 fluxes. We analyzed the effects of air temperature (T_{air}) and precipitation (P) based on the five-year average CH_4 fluxes in each region (Fig. 5).

The modeled five-year CH_4 fluxes exhibited linear trends that closely follow the trends in air temperature in Region I (Fig. 5a), Region II (Fig. 5b), Region III (Fig. 5c) and Region V (Fig. 5e), suggesting that during the past 60 years, the increased CH_4 fluxes were primarily by climate warming. The contribution of precipitation to the trends in CH_4 fluxes differed among the regions. During the past 60 years, Region I and Region III experienced large temperature increases (rates of 0.29 ℃ per decade and 0.34 ℃ per decade, respectively). These increases resulted in higher rates of increase in CH_4 fluxes, i.e., 0.67 g m^{-2} per decade (Fig. 4a) and 0.42 g m^{-2} per decade, respectively (Fig. 4c). In Region I, CH_4 fluxes were predominantly positively correlated with air temperature ($R^2=0.35$, $p<0.001$) (Fig. 5a). Although no correlation was found between the CH_4 fluxes and the precipitation in Region I, the linear precipitation decrease of 38.3 mm per decade ($p<0.001$) may have offset the increase in CH_4 fluxes due to the air temperature (Fig. 5a) before 1980. The linear precipitation decrease of 1.7 mm per decade ($p=0.4$, not significant) in Region III may also have a negative impact on CH_4 fluxes (Fig. 5c). CH_4 fluxes in Region II showed a positive

correlation with both temperature and precipitation (Fig. 5b). A slight temperature increase of 0.19 ℃ per decade and precipitation increase of 6.7 mm per decade resulted in a flux increase of 0.17 g m^{-2} per decade. In Region V, the positive correlation between CH_4 fluxes and temperature was more significant than with that of precipitation (Fig. 5e), suggesting that the temperature was the dominant factor in the acceleration of CH_4 fluxes during the past 60 years. The increase in the precipitation, at a rate of 16.6 mm per decade, although not significant (p=0.24), may have benefited the CH_4 fluxes in this region. In Region IV, CH_4 fluxes were less responsive to temperature than precipitation (Fig. 5d). The increase in temperature still promoted CH_4 fluxes to increase at a rate of 0.50 g m^{-2} per decade, although this rate was not significantly (Fig. 4d).

Interannual or interdecadal variations in CH_4 fluxes were found to be closely aligned with variations in precipitation (Fig. 5). The lowest CH_4 fluxes usually accompanied periods with low precipitation. For example, the lowest CH_4 fluxes and precipitation occurred simultaneously during the period 1980－1985 in Region IV (Fig. 5d) and the period 1965－1970 in Region V (Fig. 5e). In Region I, the five-year average CH_4 fluxes showed a trend that was synchronous with the five-year average precipitation trend (Fig. 5a), first decreasing before 1980 and then increasing until 1995. In Region I and Region II, excessive amounts of precipitation fell in the 1990s (Fig. 5a) and 2000s (Fig. 5b) in conjunction with relatively high air temperatures, which resulted in the highest CH_4 fluxes found in this study. In contrast, when the greatest amount of precipitation occurred (Fig. 5c: from 1955 to 1960 in Region III, Fig. 5d: from 1960 to 1975 in Region IV, and Fig. 5e: from 1970 to 1975 in Region V), the CH_4 fluxes remained low due to the lower air temperatures.

3.2 Changes in regional CH_4 emissions resulting from climate change and wetland loss

The total wetland area in China was approximately 35.6 million ha in 1950 (Table 1). Wetland loss was 17.0 million ha from 1950 to 2010, nearly half of the existing wetland area in 1950. During the first 50 years, wetland areas decreased by 16.1 million ha. Since 2000, wetland loss has been more limited (Table 1).

A tremendous wetland loss occurred in Region I, 7.8 million ha, accounting for approximately 45.7% of the total wetland loss (Table 1). Compared with 1950, the wetland areas decreased by 56.9%, 24.6%, 48.4%, 65.3% and 46.7% in Region I,

Region II, Region III, Region IV and Region V (Table 1), respectively.

Among the wetland types, the greatest loss occurred in inland wetlands, with a total loss of 10.3 million ha from 1950 to 2010, accounting for 60.6% of the total wetland loss. More than 95% of the inland wetland loss occurred in Region I, Region II and Region III (Table 1). In contrast, coastal wetland loss occurred primarily in eastern and southern China (Region IV and Region V) (Table 1). The coastal wetland losses were 68.5% in 2008 compared to their area in 1950. The total area loss was 4.94 million ha for lake and river wetlands between 1950 and 2008. Substantial loss of lakes/rivers occurred in eastern China (Region IV).

CH_4 emissions decreased by approximately 2.35 Tg (1.91－2.81 Tg) in China's wetlands, i.e., from 4.50 Tg in the early 1950s to 2.15 Tg in the late 2000s (Table 1). More than 99% of the CH_4 reduction occurred before 2000, which was in accordance with the wetland loss trend (Table 1).

On a national scale, the wetlands in Region I were the greatest source of the decreased CH_4 fluxes, corresponding to areas with significant wetland losses (Table 1) and the highest CH_4 fluxes (Fig. 2b). In Region I, CH_4 emissions decreased by 58.3% in the late 2000s compared with the early 1950s, with a loss of 1.68 Tg (1.36－2.03 Tg) (Table 1). In other regions, the reduction in CH_4 emissions was 0.13－0.19 Tg, with a loss fraction of 23.3－57.6% (Table 1). Among the regions, the lowest CH_4 reduction occurred in Region II, where only a slight loss in wetlands occurred. The loss fraction of CH_4 emissions was 23.3%, which is comparable to the wetland loss area (i.e., 24.6%) between 1950 and 2008 in this region (Table 1).

Methane emissions decreased by 54.4%, 62.9% and 37.1% in inland wetlands, coastal wetlands and lakes/rivers, respectively (Table 1). Region I was the most important contributor to the decreased CH_4 emissions, which contributed 85.4% to the regional CH_4 reduction for inland wetlands (Table 1). For the coastal wetlands, substantial CH_4 reduction occurred in Region V. The CH_4 fluxes decreased by nearly 82.4% from the early 1950s to the late 2000s in the coastal wetlands of this region (Table 1). Although the coastal wetland loss was higher in Region IV than in Region V, the CH_4 reduction in Region IV was only 21% of that in Region V (Table 1). This difference was because the CH_4 fluxes in the coastal wetland were 2.4 times greater in Region V than in Region IV (compare Fig. 4e with Fig. 4d).

4. Discussion

4.1 Plant growth and impacts on CH_4 emissions

Plants can enhance CH_4 production by providing methanogenic substrates and by functioning as conduits for CH_4 transport through the aerenchyma system. Conversely, plants can attenuate CH_4 emission by facilitating CH_4 oxidation through the transport and release of O_2 from roots located in anoxic peat (Whalen, 2005; Ding et al., 2005). Previous studies on pulse-labeling experiments reported a 1－3% recovery of photo-assimilated C as $^{14}CH_4$ in observational periods of 2 to 10 weeks (Wieder and Yavitt, 1994; Loya et al., 2002; King et al., 2002; King and Reeburgh, 2002). For example, King et al. (2002) estimated that more than 75% of the average CH_4 emissions from tundra wetlands originated from recently fixed carbon. However, other studies (Megonigal et al., 1996; Juutinen et al., 2003; Ding et al., 2002) have found that recent photosynthates of wetland plants provide a very limited contribution to CH_4 production, and labile organic C for CH_4 production is mainly derived from plant litter.

Many studies have indicated that most CH_4 emitted from the wetlands is mediated by aerenchymatous plants (Cicerone and Shetter, 1981; Holzapfel-Pschorn et al., 1986; Chanton et al., 1989; Waddington and Roulet, 1996). However, the ventilative and diffusive activities that transport CH_4 to the atmosphere also oxygenate the rhizosphere, creating favorable conditions for CH_4 oxidation in this otherwise anoxic, CH_4-rich zone (King 1994; Calhoun and King, 1997; 1998). The ability of aerenchymatous plants to act as a transporter differs among species (Whalen, 2005). The different transport controls may be related to plant architecture (Schimel, 1995).

The current knowledge of the effects of plants on CH_4 production and emission are insufficient and difficult to quantify for various plants. In $CH4MOD_{wetland}$, the plant-related parameters include the vegetation index (*VI*), the fraction of plant-mediated transport (T_{veg}), and the fraction of CH_4 oxidized during plant-mediated transport (P_{ox}) (Table S3). We calibrated the above parameters, focusing on sites with *Carex* and *Phragmites* (Tables S2 and S3), although these calibrations were not sufficient for use throughout the entire country. For example, mangroves are mainly species of coastal wetlands in southern China; however, we have no calibration and validation due to a lack of measurements. The plant species are abundant and diverse in Chinese wetlands (Supplementary material S3). More

experiments are needed to accurately parameterize the different plant species so that the regional estimate will be more reliable.

4.2 Variations in water table depth and the wetland extents

CH_4 fluxes are strongly controlled by the water table depth because the water table depth divides the anaerobic and aerobic zone and regulates the soil redox potential (Yu et al., 2001). Previous measurements have consistently demonstrated that CH_4 emissions decline following short- and long-term water table drawdown (Laiho, 2006; Turetsky et al., 2008). Short-term water table drawdown experiments have displayed decreased CH_4 emissions ranging from 17 to 150% depending on the extent of water table drawdown and vegetation community structure (Dise et al., 1993; Aerts and Ludwig, 1997; Strack and Waddington, 2007; Turetsky et al., 2008). Long-term (>30 year) water table drawdown studies found 67% to 96% decreases in CH_4 emissions (Yrjala et al., 2011; Nykanen et al., 1998; Ballantyne et al., 2014). Model sensitivities also show that water table depth is one of the most sensitive factors to CH_4 emissions (Boon, 1997; Zhu et al., 2013; Li et al., 2010). Thus, without proper information regarding water table positions, estimates of CH_4 are poorly constrained (Fan and Miguez-Macho, 2011).

Much progress has been made in estimating regional CH_4 emissions. However, large uncertainties remain in estimating emissions due to the spatial variability in water table depth. The TOPMODEL-based scheme (Bevenand Kirkby, 1979) has been widely used to model regional water table depth in natural wetlands (Zhu et al., 2013; Lu and Zhuang, 2012; Kleinen et al., 2012) because it is a flexible mass balance modeling tool that can be linked to biogeochemical models. TOPMODL is based on the topographic wetness index (TWI) and assumes that water tables follow topography holds (Haitjema and Mitchell-Bruker, 2005). However, the TWI is static and relies on the assumption that the local slope, i.e., $\tan\beta$, is an adequate proxy for the effective downslope hydraulic gradient, which is not necessarily true in low-relief terrain (Grabs, et al., 2009). Therefore, this algorithm is less suitable in flat areas and will induce uncertainties in the simulated water table depth. Moreover, the precision of the TWI data is important for the accuracy of the results. The HYDRO1k global values for the TWI provided by the USGS in 2000 (USGS, 2000) are the most commonly used data for the TOPMODEL method. However, the limited resolution and quality of the data can induce uncertainties, especially in tropical wetlands

(Marthews et al., 2015; Collins et al., 2011). In the future, more accurate descriptions of the hydrology process and higher-resolution datasets are needed to reduce the error in the simulated water table depth.

The definition of wetland extent is always related to water table depth. Anaerobic conditions develop when the water table is above or near the surface (within centimeters). Popular methods for defining wetland extent include using "Prescribed constant wetland extents" and the "Hydrological model" (Melton et al., 2013; Wania et al., 2013). Recently, the TOPMODEL scheme was extensively used to predict wetland distribution dynamics (Kleinen et al., 2012; Stocker et al., 2014; Melton et al., 2013). However, the simulated wetland extent will not be sensitive to the influences of anthropogenic changes to the land surface, which could lead to an overestimate of wetland area in these regions (Wania et al., 2013). In this study, we used the first method to obtain constant wetland extents for five periods (Table 1) by using remote sensing data (Niu et al., 2012). This method is simple and neglects the dynamics of wetland extent affected by climate change. However, the simulated wetland dynamics by TOPMODEL will result in large uncertainties in China, where a large area of wetlands has experienced extensive reclamation by humans. In this study, TOPMODEL was only used to predict the dynamics of water table depth inside the prescribed wetland extent. In the future, accurate simulation of the dynamics of the wetland extent affected by climate change should be considered.

4.3 Regional estimates of CH_4 emissions in Chinese wetland

Estimates of CH_4 emissions from natural wetlands in China endure large uncertainty, with the range of 1.7 Tg to 10.5 Tg from previous studies (Table 2). We estimated that the CH_4 emissions were 2.17－3.03 Tg during from 1990 to 2000, close to the lower end of the uncertainty range.

Previous studies have simply extrapolated field measurements to the national scale of China (Wang et al., 1993; 2012; Khalil et al., 1993; Jin et al., 1999; Ding et al., 2004; Chen et al., 2013; Cai, 2012) (Table 2). However, this approach may induce uncertainties because the CH_4 fluxes exhibit substantial variation according to wetland type and within different climatic and soil environments (Cao et al., 1998). For example, the estimations of both Ding et al. (2013) and Chen et al. (2004) were primarily based on measurements from Ruoergai at the eastern edge of Tibetan Plateau. However, Chen et al. (2013) used an observation of CH_4 fluxes that was

much higher than the observation of Ding et al. (2004), resulting in substantially higher emission estimates from the wetland of Tibetan Plateau (Table 2). Zhang et al. (2013) provided an estimation of 4.76 Tg CH_4 emission (Table 2) from wetlands of China with the observation of the atmospheric CH_4 concentrations, which is twice the estimated CH_4 emissions in this study. At present, the application of the top-down methods faces challenge from the spatially sparse observations of the atmospheric CH_4.

The process-based models that describe the key biogeochemical behaviors influencing the processes of CH_4 production, oxidation and emission are potentially effective tools for long-term regional estimation. Previous studies (Table 2) have focused primarily on estimating CH_4 emissions after the 1990s, except for Xu and Tian (2012) (Table 2), who inferred a reduction of approximately 1.3 Tg CH_4 from Chinese marshlands between 1949 and 2008 due to marshland conversion and climate change. But the study of Xu and Tian (2012) focused only on marshlands (natural wetlands excluding coastal wetlands, lakes and rivers), which is equivalent to the inland wetlands in this study. However, our analysis showed that the coastal wetlands, lakes and rivers represented approximately 40% of the total wetland loss (Table 1) and thus not negligible. The inclusion of the coastal wetlands, lakes and rivers consolidates the estimation of the long term changes in the CH_4 emission from wetlands on regional/national scales.

The change in wetland area is another key factors that must be considered seriously. But unfortunately, the time series of wetland changes on regional scales are often not available. The annual marshland area had been temporally interpolated using a negative correlation between the Chinese population and the marshland area of 1950 and 2000 (Liu et al., 2005; Liu and Tian, 2010). However, this relationship inevitably resulted in large uncertainties because human activity was, though important, not the only driving factor in wetland changes (Niu et al., 2012). For example, drought induced by climate warming is also the main reason for the wetland loss on Tibetan Plateau (Niu et al., 2012). We used the wetland area retrieved from remotely sensed data and the national land use data of to deduce the wetland area of differnet times (see materials and methods), which was more consolidated reliable, especially for the period after 1980. In this way, we estimated a wetland loss of 10.3 million ha and a reduction of 1.9 Tg CH_4 emission from 1950 to 2008 (Tables 1 and 2). The marshlands and wetland losses considered by Xu and Tian (2012) was only

half of this study.

Insufficient model calibration may also contribute notably to the uncertainty of the regional estimation. In North-eastern China, the dominant vegetation is *Carex*. But in Inner Mongolia, northwestern China, the North China plain and the Middle-Lower Yangtze Plain, *Phragmites* represent the primary vegetation type (see Supplementary material S3). Although *Phragmites* usually has larger biomass than *Carex*, the CH_4 fluxes are lower (according to a comparison between CH_4 fluxes in the perennial inland wetlands in WLS, ZL and SJ in Fig. S1; Table S2). If the observations of methane fluxes from the marshland dominated by *Carex* were used for the model calibration and used in the regions dominated by *Phragmites* (Xu and Tian, 2012), the national estimation mmight be overestimated. This is why the CH_4 reduction contributed 21.2% in northwestern and northern China (including Region III and Region IV in this study) in the study of Xu and Tian (2012), when the contribution was only 7.3% in this study.

There are also other factors that may introduce uncertainties into the regional estimates. Due to the high spatial heterogeneity of the wetland methane fluxes, uncertainties may be produced due to the limited resolution in the model upscaling. For example, there is substantially heterogeneity in the water table depth and the NPP at a resolution of 0.5°. Although we compared the simulated and observed CH_4 fluxes (Figures S1 and S2), the average input data of the model had inevitably omitted the heterogeneity in the CH_4 fluxes within each grid cell.

4.4 Future trends in CH_4 emissions from Chinese wetlands

According to China's National Assessment Report on Climate Change (Ding and Ren, 2007), compared with the period 1961－1990, there will be a pronounced air temperature increase of 3.6－4.9 ℃ based on the A2 and B2 scenarios (IPCC, 2000) by the end of this century in China. The precipitation is also predicted to increase by 9－11% for the A2 and B2 scenarios by 2100. The air temperature and precipitation increases differ between individual regions (Fig. 5). Depending on the regional conditions and wetland types, the consequences of future climate change on CH_4 fluxes will be spatially different and depend on regional and wetland characteristics.

Warming is expected to promote CH_4 fluxes from wetlands in the future (Zhuang et al., 2006; Christensen and Cox, 1995; Shindell et al., 2004). The air temperature is expected increase more rapidly in northeastern China (Region I), northwestern China

(Region III) and the North China Plain (the inland wetlands in Region IV) (Ding and Ren, 2007), which indicates that there will be a larger promotion of CH_4 fluxes from the inland wetlands in these regions. For the Qinghai Tibetan Plateau (Region II), eastern China (the coastal wetlands in Region IV), and southern China (Region V), the climate-induced increase in CH_4 fluxes from inland and coastal wetlands will be lower.

However, if precipitation remains unchanged, warming conditions will be accompanied by increased drought and rising sea levels (Lin et al., 2011), which will produce a negative impact on regional CH_4 emissions. For the inland wetlands, such as the marshlands of the Sanjiang Plain (Region I) and the peatlands of the Qinghai Tibetan Plateau (Region II), drought conditions will increase evapotranspiration, decrease the anti-interference ability of wetlands, speed up wetland degradation (Liu et al., 2001), and ultimately decrease CH_4 fluxes and regional CH_4 emissions in the future. For the lakes and rivers, drought is expected to reduce the lake areas (Yu et al., 2004) and decrease regional CH_4 emissions in northeastern China (Region I) and Inner Mongolia. Although short-term expansion in the lakes may occur because of glacial melting over the western plateau of China (Region II and western Region III), water shortages will result in the long-term disappearance of the lakes (Shen et al., 2003a). Fortunately, precipitation is expected to increase, especially in northern China (Region I, Region III and the inland wetlands in Region IV) and on the Qinghai Tibetan Plateau (Region IV) (Ding and Ren, 2007), which may offset the negative impact on CH_4 emissions from the inland wetlands and lakes by the imminent drought conditions. For the coastal wetlands, rising sea levels will reduce the area of coastal wetlands by inundation. Consider the Jiangsu Province in eastern China (Region IV) as an example, where 396, 617 and 1390 km^2 is expected to be lost in the next 30, 50 and 100 years, respectively (Li et al., 2006). Moreover, rising sea levels will increase the invasion of salt water to estuarine wetlands (Shen et al., 2003b; Hu et al., 2003; Huang and Xie, 2000), which will reduce CH_4 fluxes due to the higher salinity.

4.5 Present state and future challenges in the CH_4 modeling

Matthews and Fung (1987) began modeling wetland methane using vegetation, soil and fractional inundation maps, which led to process based modeling of CH_4 production, oxidation and transport (Cao et al., 1996; Walter et al., 1996; Potter et al., 1997; Zhang et al., 2002). Recently, the WETCHIMP project (Wetland CH_4 Inter-comparison of Models Project) evaluated the present ability to simulated

large-scale CH_4 emissions from wetlands. In this study, the $CH4MOD_{wetland}$ and WETCHIMP models, e.g., CLM4Me (Rieley et al., 2011), LPJ-WhyMe (Wania et al., 2010), DLEM (Tian et al., 2010; Xu et al., 2010), ORCHIDEE (Krinner et al., 2005), SDGVM (Woodward et al., 1995; Beerling and Woodward, 2001), are all process-based models used for simulating CH_4 production, oxidation and transport. In $CH4MOD_{wetland}$, the methanogenic substrates include root exudates, plant litter and soil organic matter. This is similar to those of the LPJ-WhyMe model. DLEM only considers CH_4 production from dissolved organic carbon (DOC). In CLM4Me, CH_4 production is related to the heterotrophic respiration from soil and litter. ORCHIDEE uses a fraction of the most labile "Litter + soil C" pool. In most of the models, the methane production rates are determined by the availability of methanogenic substrates and the influence of environmental factors, including soil temperature, soil texture, redox potential and pH. LPJ-WhyMe does not consider the influences of redox potential and pH because Wania et al. (2010) reported that the pH and redox factors should be excluded because they are poorly characterized. However, Riley et al. (2011) considered pH and redox potential in the CLM4Me model. We considered the influence of redox potential but not pH in the $CH4MOD_{wetland}$ model. The $CH4MOD_{wetland}$ model assigned a fixed proportion of CH_4 oxidation during transport through the plant and by diffusion, which was similar to the method used in the DLEM, SDGVM and ORCHIDEE models. However, the CLM4Me and LPJ-WHyMe models illustrated the process of CH_4 oxidation explicitly. For example, CLM4Me used the Michaelis-Menten kinetics equation (Arah and Stephen, 1998; Segers, 1998) to calculate the CH_4 oxidation rate.

In the models considered in this study, the intra-annual or inter-annual CH_4 emission trends are largely influenced by the soil temperature, NPP and water table depth. The simulated seasonal variations of the CH_4 fluxes from the sites match the observed values well (Fig. S1). The lowest CH_4 fluxes occurred during the winter or dry period, and the highest fluxes appeared during the summer and flooding period (Fig. S1). The intra-annual variations in this study (Fig. 3) are similar to the simulated seasonal cycles in West Siberia (Bohn et al., 2015) or the northern Hemisphere (Melton et al., 2013), which peak in July or August and are mainly driven by high temperature and NPP. In this study, the simulated mean CH_4 flux during the winter in northeastern China (0.5 mg m^{-2} h^{-1}, Fig. 3a) is similar to the observations from the

Carex lasiocarpa site in the Sanjiang Plain (Zhang et al., 2004). Yang et al. (2004) reported that the fractions of CH_4 flux in the winter and freeze-thaw period were 2.2%—5.5% and 20.6—30.8%, respectively. In this study, the simulated CH_4 fluxes in the winter and freeze-thaw period accounted for ~8.6% and ~21.1% in Region I, respectively (Fig. 3a). The simulated CH_4 fluxes increased by ~8% during the past 60 years (Fig. 4f) and were driven by climate in this study. This increase is similar to the increase observed by Zhuang's (Zhuang et al., 2004), who reported a CH_4 emissions increase of ~7% between the 1950s and 2000s in the Pan-Arctic region.

Although recently developed process-based CH_4 models have become more specialized to adequately represent CH_4 production, oxidation, and transport by considering various factors and controls, a knowledge gap still exists regarding CH_4 modeling (Bridgham et al., 2013). One example of an insufficiently modeled process is the influence of thawing permafrost on CH_4 production in the arctic region. Lacking thawing, freezing and snow melting processes will result in distorted CH_4 simulations during the winter and freeze-thaw period. In addition, the dynamics of some important factors, such as soil pH, Eh and Q_{10}, were modeled using simple functions or as a constant in the models considered in this study. For example, Q_{10} was defined as a constant of 3.0 in the $CH4MOD_{wetland}$ model. However, the reported Q_{10} values for methanogens in wetland soils vary widely (1—35) (Whalen, 2005); thus, using a constant value will inevitably result in uncertainties in the simulation. The uncertainties of quantifying large-scale CH_4 emissions usually result from rough characterization of vegetation conditions and poor global distribution of wetlands and lakes. The vegetation parameters in CH_4 models usually refer to the production of labile organic compounds from gross primary production (GPP) and the transport of CH_4 to the atmosphere via plant stems and leaves. These vegetation parameters are different between plant species but are usually unified in regional simulations. Large differences exist between the distribution and extent of global wetlands and lakes, regardless of whether the "Prescribed constant wetland extents", "Remotely-sensed inundation" or "Hydrological model" are used (Melton et al., 2013). All of these methods can result in large uncertainties in simulated regional CH_4 emissions. Future work is greatly needed to focus on the above uncertainties and to accurately estimate regional CH_4 emissions.

5. Conclusions

Climate warming increased CH_4 fluxes at a rate of 0.52 g m^{-2} per decade from 1950 to 2010. However, during the same period, an estimated 2.35 Tg (1.91－2.81 Tg) of CH_4 reduction in Chinese wetlands occurred, which was mainly due to extensive wetland loss, i.e., from 35.6 million ha to 18.6 million ha. On a national scale, northeastern China experienced a large temperature increase, which resulted in the highest rate of increase in CH_4 fluxes, i.e., 0.67 g m^{-2} per decade. However, serious wetland loss made northeastern China become the greatest source of CH_4 decrease, accounting for 70% of the total CH_4 reduction. The Qinghai Tibetan Plateau had the lowest CH_4 reduction, which was approximately 8% of the reduction in northeastern China. Among the reduction, the inland wetlands, lakes/rivers and the coastal wetlands accounted for 81%, 11% and 8%, respectively.

Author contribution

T. L., W. Z., T. V. and M. R. designed the research; Q. Z. and G. W. performed the CH_4 modeling; Y. L. performed the TEM modeling; Z. N. performed the wetland area analysis.

Acknowledgements

This work was supported by the National Natural Science Foundation of China (Grant No. 31000234, 41321064 and 41175132), the Chinese Academy of Sciences (CAS) strategic pilot technology special funds (Grant No. XDA05020204), the Academy of Finland Center of Excellence (Grants No. 1118615 and 272041), ICOS 271878, ICOS-Finland 281255, ICOS-ERIC 281250, Academy Professor projects (1284701 and 1282842) and the Nordic Centre of Excellence DEFROST. We are grateful to Professor Yao Huang in the Institute of Botany, Chinese Academy of Science to provide the valuable recommendations and opinions to this paper. We would also like to thank the Pan-Eurasian Experiment (PEEX)

References

Aerts, R. and Ludwig, F.: Water-table changes and nutritional status affect trace gas emissions from laboratory columns of peatland soils, Soil Biol. Biochem., 29, 1691-1698, 1997.

An, S. Q., Li, H. B., Guan, B. H., Zhou, C. F., Wang, Z. S., Deng, Z. F., Zhi, Y. B., Liu, Y. L., Xu, C., Fang, S. B., Jiang, J. H., and Li, H. L.: China's natural wetlands: past problems, current status, and future challenges, Ambio, 36, 335-342, 2007.

Antonov, J. I., Seidov, D., Boyer, T. P., Locarnini, R. A., Mishonov, A. V., Garcia, H. E., Baranova, O. K., Zweng, M. M. and Johnson, D. R.: World Ocean Atlas 2009 Vol. 2, Salinity, in: NOAA Atlas NESDIS 69, edited by: Levitus, S., US Government Printing Office, Washington, D.C., 1-184, 2010.

Arah, J. R. M. and Stephen, K. D.: A model of the processes leading to methane emission from peatland, Atmos. Environ., 32, 3257– 3264, 1998.

Ballantyne, D. M., Hribljan, J. A., Pypker, T. G. and Chimner, R. A.: Long-term water table manipulations alter peatland gaseous carbon fluxes in Northern Michigan, Wetl. Ecol. Manag., 22, 35-47, 2014.

Beerling, D. J. and Woodward, F. I.: Vegetation and the Terrestrial Carbon Cycle: Modelling the first 400 Million Years, Cambridge University Press, Cambridge, 2001.

Beven, K. J. and Kirkby, M. J.: A physically based, variable contributing area model of basin hydrology, Hydrolog. Sci. Bull., 24, 43-69, 1979.

Belward, A. S., Estes, J. E. and Kline, K. D.: The IGBP-DIS global 1-km land-cover data set DISCover: A project overview, Photogramm. Eng. Rem. S., 65, 1013-1020, 1999.

Bohn, T. J., Lettenmaier, D. P., Sathulur, K., Bowling, L. C., Podest, E., McDonald, K. C. and Friborg, T.: Methane emissions from western Siberian wetlands: heterogeneity and sensitivity to climate change, Environ. Res. Lett., 2, 045015 doi:10.1088/1748-9326/2/4/045015, 2007.

Bohn, T. J., Melton, J. R., Ito, A., Kleinen, T., Spahni, R., Stocker, B. D., Zhang, B., Zhu, X., Schroeder, R., Glagolev, M. V., Maksyutov, S., Brovkin, V., Chen, G., Denisov, N. S., Eliseev, A. V., Gallego-Sala, A., McDonald, K. C., Rawlins, M. A., Riley, W. J., Subin, Z. M., Tian, H., Zhuang, Q., and Kaplan, J. O.: WETCHIMP-WSL: intercomparison of wetland methane emissions models over West Siberia, Biogeosciences, 12: 3321-3349, 2015.

Boon, P. I., Mitchell, A. and Lee, K.: Effects of wetting and drying on methane emissions from ephemeral floodplain wetlands in southeastern Australia, Hydrobiologia, 357, 73-87, 1997.

Bridgham, S. D., Cadillo-Quiroz, H., Keller, J. K., and Zhuang, Q. L.: Methane

emissions from wetlands: biogeochemical, microbial, and modeling perspectives from local to global scales, Glob. Change Biol., 19(5): 1325-1346, 2013.

Cai, Z. C.: Greenhouse gas budget for terrestrial ecosystems in China, Sci. China Earth Sci., 55, 173-182, 2012.

Calhoun, A. and King, G. M.: Regulation of rootassociated methanotrophy by oxygen availability in the rhizosphere of two aquatic macrophytes, Appl. Environ. Microb., 63, 3051-3058, 1997.

Calhoun, A. and King, G. M.: Characterization of root-associated methanotrophs from three freshwater macrophytes: Pontederia cordata, Sparganium eurycarpum, and Sagittaria latifolia, Appl. Environ. Microb., 64, 1099-1105, 1998.

Cao, M. K., Marshall, S., and Gregson, K.: Global carbon exchange and methane emissions from natural wetlands: Application of a process-based model, J. Geophys. Res.-Atmos., 101, 14399– 14414, 1996.

Cao, M. K., Gregson, K. and Marshall, S.: Global methane emission from wetlands and its sensitivity to climate change, Atmos. Environ., 32, 3293-3299, 1998.

Chanton, J. P., Martens, C. S. and Kelley, C. A.: Gas transport from methane-saturated, tidal freshwater and wetland sediments, Limnol. Oceanogr., 34, 807-819, 1989.

Chen, H., Zhu, Q., Peng, C. H., Wu, N., Wang, Y. F., Fang, X. Q., Jiang, H., Xiang, W. H., Chang, X., Deng, X. W. and Yu G. R.: Methane emissions from rice paddies natural wetlands, lakes in China: synthesis new estimate, Glob. Change Biol., 19, 19-32, 2013.

Christensen, T. and Cox, P.: Response of methane emission from arctic tundra to climate change: results from a model simulation, Geophys. Res. Lett., 31, L04501, doi:10.1029/2003GL018680, 1995.

Christensen, T. R., Ekberg, A., Strom, L., Mastepanov, M., Panikov, N., Öquist, M., Svensson, B. H., Nykänen, H., Martikainen, P. J. and Oskarsson, H.: Factors controlling large scale variations in methane emissions from wetlands, Geophys. Res. Lett., 30, 1414, doi:10.1029/2002GL016848, 2003.

Cicerone, R. J. and Shetter, J. D.: Sources of atmospheric methane: measurements in rice paddies and a discussion, J. Geophys. Res., 86, 7203-7209, 1981.

Collins, W., Bellouin, N., Doutriaux-Boucher, M., Gedney, N., Halloran, P., Hinton, T., Hughes, J., Jones, C. D., Joshi, M., Liddicoat, S., Martin, G., O'Connor, F., Rae, J., Senior, C., Sitch, S., Totterdell, I., Wiltshire, A. and Woodward, S.: Development and evaluation of an Earth-system model-HadGEM2, Geosci.

Model Dev., 4, 1051-1075, 2011.

Cramer, W., Kicklighter, D. W., Bondeau, A., Moore Iii, B., Churkina, G., Nemry, B., Ruimy, A., Schloss, A. L., and The Participants of the Potsdam NPP Model Intercomparison: Comparing global models of terrestrial net primary productivity (NPP): overview and key results, Glob. Change Biol., 5, 1-15, 1999.

Denman, K. L., Brasseur, G., Chidthaisong, A., Ciais, P., Cox, P. M., Dickinson, R. E., Hauglustaine, D., Heinze, C., Holland, E., Jacob, D., Lohmann, U., Ramachandran, S., da Silva Dias, P. L., Wofsy, S. C., and Zhang, X.: Couplings between changes in the climate system and biogeochemistry, in: Climate Change 2007: The Physical Science Basis. Contribution of Working Group I to the Fourth Assessment Report of the Intergovernmanetal Panel on Climate Change, edited by: Solomon, S., Qin, D., Manning, M., Chen, Z., Marquis, M., Averyt, K. B., Tignor, M. and Miller, H. L., Cambridge University Press, Cambridge, 539-544, 2007.

Ding, W. X., Cai, Z. C., Tsuruta, H. and Li, X. P.: Effect of standing water depth on methane emissions from freshwater marshes in northeast China, Atmos. Environ., 36, 5149-5157, 2002.

Ding, W., X., Cai, Z. and Wang, D.: Preliminary budget of methane emissions from natural wetlands in China, Atmos. Environ., 38, 751-759, 2004.

Ding, W., X., Cai, Z. and Tsuruta, H.: Factors affecting seasonal variation of methane concentration in water in a freshwater marsh vegetated with *Carex lasiocarpa*, Biol Fertil Soils, 41, 1-8, 2005.

Ding, W. X. and Cai, Z. C.: Methane emission from natural wetlands in China: summary of years 1995-2004 studies, Pedosphere, 17, 475-486, 2007.

Ding, Y. H. and Ren, G. Y.: Climate change in China and its future trend, in: National assessment report of climate change, edited by: editing committee of national assessment report of climate change, Science Press, China, 130-161, 2007. (in Chinese with English abstract)

Dise, N. B., Gorham, E. and Verry, E. S.: Environmental factors controlling methane emissions from peatlands in Northern Minnesota, J. Geophys. Res. Atmos., 98, 10.583-10.584, D6. doi:10.1029/93JD00160, 1993.

Du, X. and Chen, W.: Towards a better understanding of modeling feasibility robustness in engineering design, in: 1999 ASME design technical conference, paper No. DAC-8565, Las Vegas, Nevada, September 1999.

Fan, Y. and van den Dool, H.: Climate prediction center global monthly soil moisture data set at 0.5 ° resolution for 1948 to present, J. Geophys. Res., 109, D10102, doi:10.1029/2003JD004345, 2004.

Fan, Y. and Miguez-Macho, G.: A simple hydrologic framework for simulating wetlands in climate and earth system models, Clim. Dynam., 37, 253-278, 2011.

FAO/IIASA/ISRIC/ISS-CAS/JRC: Harmonized World Soil Database, version 1.0, FAO, Rome,Italy and IIASA, Laxenburg, Austria, 2008.

FAO/IIASA/ISRIC/ISSCAS/JRC: Harmonized World Soil Database, version 1.2, FAO and IIASA, Rome, Italy and Laxenburg, Austria, 2012.

Forster, P., Ramaswamy, V., Artaxo, P., Berntsen, T., Betts, R., Fahey, D., Haywood, J., Lean, J., Lowe, D., Myhre, G., Nganga, J., Prinn, R., Raga, G., Schulz, M. and Van Dorland, R.: Changes in atmospheric constituents and in radiative forcing, in: Climate Change 2007: The Physical Science Basis. Contribution of Working Group I to the Fourth Assessment Report of the Intergovernmental Panel on Climate Change, edited by: Solomon, S., Qin, D., Manning, M., Chen, Z., Marquis, M., Averyt, K. B., Tignor, M. and Miller, H. L., Cambridge University Press, Cambridge, 131-243, 2007.

Gill, R. A. and Jackson, R. B.: Global patterns of root turnover for terrestrial ecosystems, New Phytol., 147, 13-31, 2000.

Gill, R. and Jackson, R. B.: Global Distribution of Root Turnover in Terrestrial Ecosystems, Oak Ridge National Laboratory Distributed Active Archive Center, Oak Ridge, Tennessee, U.S.A. doi:10.3334/ORNLDAAC/661, 2003.

Grabs, T., Seibert, J., Bishop, K. and Laudon, H.: Modeling spatial patterns of saturated areas: A comparison of the topographic wetness index and a dynamic distributed model, J. Hydrol., 373, 15-23, 2009.

Haitjema, H. M. and Mitchell-Bruker, S.: Are water tables a subdued replica of the topography? Ground Water, 43, 781-786, 2005.

Harris, I., Jones, P. D., Osborn, T. J. and Lister, D. H.: Updated high-resolution grids of monthly climatic observations-the CRU TS3.10 Dataset, Int. J. Climatol., 1, doi: 10.10, 2014.

Holzapfel-Pschorn, A., Conrad, R. and Seiler, W.: Effects of vegetation on the emission of methane from submerged paddy soil, Plant Soil, 92, 223-233, 1986.

Huang, Y., Sass, R. L. and Fisher, F. M.: A semi-empirical model of methane emission from flooded rice paddy soils, Glob. Change Biol., 4, 247–268, 1998.

Huang, Y., Zhang, W., Zheng, X., Li, J. and Yu, Y.: Modeling methane emission from rice paddies with various agricultural practices, J. Geophys. Res., 109, D08113, doi: 10.1029/2003JD004401, 2004.

Huang, Y., Zhang, W., Zheng, X., Han, S. and Yu, Y.: Estimates of methane emissions from Chinese rice paddies by linking a model to GIS database, Acta Ecologica Sinica, 26, 980–987, 2006.

Huang, Y., Sun, W., Zhang, W., Yu, Y. Q., Su, Y. H. and Song, C. C. Marshland conversion to cropland in northeast China from 1950 to 2000 reduced the greenhouse effect, Glob. Change Biol., 16, 680-695, 2010.

Huang, Z. G. and Xie, X. D.: Change of the sea level and its effect and countermeasures, Guangdong science and Technology Press, China, 2000.

Hu, S., Zhu, J. R., Fu, D. J. and Wu, H.: Estuarine circulation and saltwater intrusion II: impacts of river discharge and rise of sea level, Journal of Ocean University of Qingdao, 33, 337-342, 2003. (in Chinese with English abstract)

IPCC: Emission Scenarios: A Special Report of Workgroup III of IPCC. Cambridge University Press, UK, 2000.

IPCC: Climate Change 2007: The Physical Science Basis. Contribution of Working Group I to the Fourth Assessment Report of the Intergovernmental Panel on Climate Change, edited by: Solomon, S., Qin, D., Manning, M., Chen, Z., Marquis, M., Averyt, K. B., Tignor, M. and Miller, H. L.). Cambridge University Press, Cambridge, 2007.

IPCC: Climate Change 2013: The Physical Science Basis. Contribution of Working Group I to the Fifth Assessment Report of the Intergovernmental Panel on Climate Change, edited by: Stocker, T. F., Qin, D., Plattner, G. K., Tignor, M., Allen, S. K., Boschung, J., Nauels, A., Xia, Y., Bex, V. and Midgley, P. M., Cambridge University Press, Cambridge, 2013.

Jin, H. J., Wu, J., Cheng, G. D., Tomoko, N. and Sun, G. Y.: Methane emissions from wetlands on the Qinghai-Tibet Plateau, Chinese Sci. Bull., 44, 2282-2286, 1999.

Juutinen, S., Larmola, T., Remus, R., Mirus, E., Merebach, W., Silvola, J. and Augustin, J.: The contribution of *Phragmites australis* litter to methane emission in planted and non-planted fen microcosms, Biol. Fert. Soils, 38, 10-14, 2003.

Khalil, M. A. K., Shearer, M. J. and Rasmussen, R. A.: Methane sources in China: historical and current emissions, Chemosphere, 26, 127-142, 1993.

King, G. M.: Associations of methanotrophs with roots and rhizomes of aquatic

vegetation, Appl. Environ. Microb., 60, 3220-3227, 1994.

King, J. Y. and Reeburgh, W. S.: A pulse-labeling experiment to determine the contribution of recent plant photosynthates to net methane emission in arctic wet sedge tundra, Soil Biol. Biochem., 34, 173-180, 2002.

King, J. Y., Reeburgh, W. S., Thieler, K. K., Kling, G. W., Loya,W. M., Johnson, L. C. and Nadelhoffer, K. J.: Pulse-labeling studies of carbon cycling in Arctic tundra ecosystems: The contribution of phytosynthates to methane emission, Global Biogeochem. Cy., 16, 1062, doi:10.1029/2001GB001456, 2002.

Kleinen, T., Brovkin, V. and Schuldt, R. J.: A dynamic model of wetland extent and peat accumulation: results for the Holocene, Biogeosciences, 9, 235-248, 2012.

Krinner, G., Viovy, N., de Noblet-Ducoudre, N., Ogee, J., Polcher, J., Friedlingstein, P., Ciais, P., Sitch, S., and Prentice, I. C.: A dynamic global vegetation model for studies of the coupled atmosphere-biosphere system, Global Biogeochem. Cy., 19, 941–962, 2005.

Laiho, R.: Decomposition in peatlands: reconciling seemingly contrasting results on the impacts of lowered water levels, Soil Biol. Biochem., 38, 2011-2024, 2006.

Lang, H. Q. and Zu, W. C.: Marshland in Chinese, Shandong Science and Technology Press, China, 1983.

Li, J. L., Wang, Y. H., Zhang, R. S., Qi, D. L. and Zhang, D. F.: Disaster effects of sea level rise - a case of Jiangsu coastal low land, Sci. Geograph. Sinica, 26, 87-93, 2006. (in Chinese with English abstract)

Li, T., Huang, Y., Zhang, W. and Song, C.: CH4MOD$_{wetland}$: A biogeophysical model for simulating CH_4 emissions from natural wetland, Ecol. Model., 221, 666-680, 2010.

Li, T., Huang, Y., Zhang, W. and Yu, Y.: Methane emissions associated with the conversion of marshland to cropland and climate change on the Sanjiang Plain of northeast China from 1950 to 2100, Biogeosciences, 9, 1-17, 2012.

Lin, E. D., Wu, S. H. and Luo, Y.: Climate change impacts and adaptation, in: The second national assessment report of climate change, edited by: editing committee of the second national assessment report of climate change, Science Press, China, 195-339, 2011. (in Chinese with English abstract)

Liu, J., Tian, H., Liu, M., Zhuang, D., Melillo, J. M. and Zhang, Z.: China's changing landscape during the 1990s: Large‐scale land transformations estimated with

satellite data, Geophys. Res. Lett., 32, L02405, doi:10.1029/2004GL021649, 2005.

Liu, M. and Tian, H.: China's land cover and land use change from 1700 to 2005: Estimations from high-resolution satellite data and historical archives, Global Biogeochem. Cy., 24, GB3003, doi:10.1029/2009GB003687, 2010.

Liu, X. T. and Ma, X. H.: Influence of large scale reclamation on natural environment and regional environmental protection in the Sanjiang Plain, Sci. Geograph. Sinica, 20, 14-19, 2000. (in Chinese with English abstract)

Liu, Z. Q., Liu, H. Y. and Lv, X. G.: Ecological fragility of wetlands in Sanjiang Plain, Chinese J. Appl. Ecol., 12, 241-244, 2001. (in Chinese with English abstract)

Loya, W. M., Johnson, L. C., Kling, G. W., King, J. Y., Reeburgh, W. S. and Nadelhoffer, K. J.: Pulse-labeling studies of carbon cycling in arctic tundra ecosystems: Contribution of photosynthesis to soil organic matter, Global Biogeochem. Cy., 16, 1101, doi:10.1029/2001GB001464, 2002.

Loveland, T. R., Brown, J. F., Ohlen, D. O., Zhu, Z., Yang, L., Merchant, J. W. and Reed, B. C.: Development of a global land cover characteristics database and IGBP DISCover from 1 km AVHRR data, Int. J. Remote Sens., 21, 1303-1330, 2000.

Lu, X. and Zhuang, Q.: Modeling methane emissions from the Alaskan Yukon River basin, 1986-2005, by coupling a larg-scale hydrological model and a process-based methane model, J. Geophys. Res., 117, G02010, doi:10.1029/2011JG001843, 2012.

Marthews, T., Dadson, S., Lehner, B., Abele1, S. and Gedney, N.: High-resolution global topographic index values for use in large-scale hydrological modeling, Hydrol. Earth Syst. Sc., 19, 91-104, 2015.

Matthews, E. and Fung, I. Y.: Methane emission from natural wetlands: Global distribution, area, and environmental characteris characteristics of sources, Global Biogeochem. Cy., 1, 61–86, 1987.

McGuire, A. D., Melillo, J. M., Joyce, L. A., Kicklighter, D. W., Grace, A. L., Moore III, B. and Vorosmarty, C. J.: Interactions between carbon and nitrogen dynamics in estimating net primary productivity for potential vegetation in North America, Global Biogeochem. Cy., *6*(2), 101-124, 1992.

Megonigal, J. P., Whalen, S. C., Tissue, D. T., Bovard, B., Allen, A., Alberts, D. and Schlesinger, W. H.: The use $^{14}CO_2$ to trace carbon metabolism from

photosynthesis through methanogenesis in a wetland plant-soil-atmosphere microcosm, Fourth Symposium on Biogeochemistry of Wetlands, New Oreleans, Louisiana, UAS, 1996, pp 21-31.

Melillo, J. M., Mcguire, A. D., Kicklighter, D. W., Moore, B., Vorosmarty, C. J. and Schloss, A. L.: Global climate change and terrestrial net primary production, Nature, 363, 234-240, 1993.

Melton, J., Wania, R., Hodson, E. L., Poulter, B., Ringeval, B., Spahni, R., ,Bohn, T., Avis, C. A.,Beerling, D. J., Chen, G., Eliseev, A. V., Denisov, S. N., Hopcroft, P. O., Lettenmaier, D. P., Riley, W. J., Singarayer, J. S., Subin, Z. M.,Tian, H., Zurcher, S., Brovkin, V., van Bodegom, P. M., Kleinen, T., Yu, Z. C.,and Kaplan : Present state of global wetland extent and wetland methane modelling: conclusions from a model intercomparison project (WETCHIMP), Biogeosciences 10: 753-788, 2013.

Mitsch, J. W. and Gosselink, J. G.: Wetlands, 4th edn. JohnWiley and Sons Inc, Hoboken, NJ, 2007.

Moser, M., Prentice, C. and Frazier, S.: A global overview of wetland loss and degradation. Proceedings to the 6th Meeting of the Conference of Contracting Parties of the Ramsar Convention, Brisbane, Australia, Vol. 10/12B, 21-31, March 1996.

Niu, Z. G., Zhang, H. Y., Wang, X. W., Yao W. B., Zhou, D. M., Zhao, K. Y., Zhao, H., Li, N. N., Huang, H. B., Li, C. C., Yang, J., Liu, C. X., Liu, S., Wang, L., Li, Z., Yang, Z. Z., Qiao, F., Zheng, Y. M., Chen, Y. L., Sheng, Y. W., Gao X. H., Zhu, W. H., Wang, W. Q., Wang, H., Weng, Y. L., Zhuang, D. F., Liu, J. Y., Luo, Z. C., Cheng, X., Guo, Z. Q. and Gong, P.: Mapping wetland changes in China between 1978 and 2008, Chinese Sci. Bull., 57, 2813-2823, 2012.

Nisbet, E. G., Dlugokencky, E. J. and Bousquet, P.: Methane on the rise-again. Science, 343, 493-495, 2014.

Nykanen, H., Alm, J., Silvola, J., Tolonen, K. and Martikainen, P. J.: Methane fluxes on boreal peatlands of different fertility and the effect of long-term experimental lowering of the water table on flux rates, Global Biogeochem. Cy., 12, 53-69, 1998.

Potter, C.: An ecosystem simulation model for methane production and emission from wetlands, Global Biogeochem. Cy., 11, 495– 506, 1997.

Potter, C., Klooster, S., Hiatt, S., Fladeland, M., Genovese, V. and Gross, P.: Methane

emissions from natural wetlands in the United States: satellite-derived estimation based on ecosystem carbon cycling, Earth Interact., 10, 1-12, 2006.

Revenga, C., Brunner, J., Henninger, N., Kassem, K. and Payne, R.: Pilot Analysis of Global Ecosystems: Freshwater Systems, World Resources Institute, Washington, DC, 2000.

Riley, W., Subin, Z. M., Lawrence, D. M., Swenson, S. C., Torn, M. S., Meng, L., Mahowald, N. M., and Hess, P.: Barriers to predicting changes in global terrestrial methane fluxes: analyses using CLM4Me, a methane biogeochemistry model integrated in CESM, Biogeosciences, 8(7), 1925-1953, 2011.

Schimel, J. P.: Plant transport and methane production as controls on methane flux from arctic wet meadow tundra, Biogeochemistry, 28, 183-200, 1995.

Segers, R.: Methane production and methane consumption: a review of processes underlying wetland methane fluxes, Biogeochemistry, 41, 23–51, 1998.

Shindell, D. T., Walter, B. P. and Faluvegi, G.: Impacts of climate change on methane emissions from wetlands, Geophys. Res. Lett., 31, L21202, doi:10.1029/2004GL021009, 2004.

Shindell, D. T., Faluvegi, G., Koch, D. M., Schmidt, G. A., Unger, N. and Bauer, S. E.: Improved attribution of climate forcing to emissions, Science, 326, 716-718, 2009.

Shen, Y. P., Liu, S. Y., Ding, Y. J. and Wang, S. D.: Glacier mass balance change in Tailanhe river watersheds on the south slope of the Tianshan Mountains and its impact on water resources, Journal of Glaciology Geocryology, 25, 124-129, 2003a. (in Chinese with English abstract)

Shen, H. T., Mao, Z. C. and Zhu, J. R.: Salt water intrusion in Changjiang Estuary, China Ocean Press, China, 2003b. (in Chinese with English abstract)

Stocker, B. D., Spahni, R., and Joos, F.: DYPTOP: a costefficient TOPMODEL implementation to simulate sub-grid spatio-temporal dynamics of global wetlands and peatlands, Geosci. Model Dev., 7, 3089–3110, doi:10.5194/gmd-7-3089-2014, 2014.

Strack, M. and Waddington, J. M.: Response of peatland carbon dioxide and methane fluxes to a water table drawdown experiment, Global Biogeochem. Cy., 21, GB1007. doi:10.1029/2006GB002715, 2007.

Tian, H., Xu, X., Liu, M., Ren,W., Zhang, C., Chen, G., and Lu, C.: Spatial and temporal patterns of CH4 and N2O fluxes in terrestrial ecosystems of North

America during 1979–2008: application of a global biogeochemistry model, Biogeosciences, 7, 2673–2694, doi:10.5194/bg-7-2673-2010, 2010.

Tian, H., Xu, X., Lu, C., Liu, M. L., Ren, W., Chen, G. S., Melillo, J. and Liu, J. Y.: Net exchanges of CO_2, CH_4, and N_2O between China's terrestrial ecosystems and the atmosphere and their contributions to global climate warming, J. Geophys. Res., 116, G02011, doi:10.1029/2010JG001393, 2011.

Turetsky, M. R., Treat, C. C., Waldrop, M. P., Waddington, J. M., Harden, J. W. and McGuire, A. D.: Short-term response of methane fluxes and methanogen activity to water table and soil warming manipulations in an Alaskan peatland, J. Geophys. Res., 113, G00A10. doi:10.1029/2007JG000496, 2008.

USGS: US Geological Survey: HYDRO1k Elevation derivative database, US Geological Survey Earth Resources Observation and Science (EROS) Center, Sioux Falls, South Dakota, 2000.

Wania, R., Ross, I., and Prentice, I. C.: Implementation and evaluation of a new methane model within a dynamic global vegetation model: LPJ-WHyMe v1. 3.1, Geoscientific Model Development 3(2), 565-584, 2010.

Wania, R., Melton, J. R., Hodson, E. L., Poulter, B., Ringeval, B., Spahni, R., Bohn, T., Avis, C. A., Chen, G., Eliseev, A. V., Hopcroft, P. O., Riley, W. J., Subin, Z. M., Tian, H., van Bodegom, P. M., Kleinen, T., Yu, Z. C., Singarayer, J. S., Zürcher, S., Lettenmaier, D. P., Beerling, D. J., Denisov, S. N., Prigent, C., Papa, F., and Kaplan, J. O.: Present state of global wetland extent and wetland methane modelling: methodology of a model inter-comparison project (WETCHIMP), Geoscientific Model Development, 6(3), 617-641, 2013.

Walter, B. P., Heimann, M., Shannon, R. D., and White, J.: A process-based model to derive methane emissions from natural wetlands, Geophys. Res. Lett., 23, 3731–3734, 1996.

Walter, B. P. and Heimann, M.: A process-based, climate-sensitive model to derive methane emissions from natural wetlands: application to five wetland sites, sensitivity to model parameters, and climate. Global Biogeochem. Cycles, 14 (3), 745–765, 2000.

Wang, M. X., Dai, A. G., Huang, J., Ren, L. X. and Shen, R. X.: Sources of methane in China: rice fields, agricultural waste treatment, cattle, coal mines, and other minor sources, Scientia Atmospherica Sinica, 17, 52-64, 1993. (in Chinese with English abstract)

Wang, X. K., Lu, F. and Yang, L.: Methane emissions from China's natural wetlands: measurements, temporal variations and influencing factors, in: Recarbonization of the Biosphere, edited by: Lal, R., Lorenz, K., Hüttl, R. F., Schneider, B. U. and von Braun, J., Springer Netherlands, 99-125, 2012.

Waddington, J. M. and Roulet, N. T.: Atmosphere-wetland carbon exchanges: scale dependency of CO_2 and CH_4 exchange on the developmental topography of a peatland, Global Biogeochem. Cy., 10, 233-245, 1996.

Whalen, S. C.: Biogeochemistry of methane exchange between natural wetlands and the atmosphere, Environ. Eng. Sci., 22, 73-94, 2005.

Wieder, R. K., Yavitt, J. B.: Peatlands and global climate change: Insights from comparative studies of sites situated along a latitudinal gradient, Wetlands, 14, 229-238, 1994.

Woodward, F. I., Smith, T. M., and Emanuel, W. R.: A global land primary productivity and phytogeography model, Global Biogeochem.Cy., 9, 471–490, 1995.

Xu, X. F., Tian, H. Q., Zhang, C., Liu, M. L., Ren, W., Chen, G. S., Lu, C. Q., and Bruhwiler, L.: Attribution of spatial and temporal variations in terrestrial methane flux over North America, Biogeosciences, 7, 3637–3655, doi:10.5194/bg-7-3637-2010, 2010.

Xu, X. and Tian, H.: Methane exchange between marshland and the atmosphere over China during 1949-2008, Global Biogeochem. Cy., 26, GB2006, doi:10.1029/2010GB003946, 2012.

Yang, W. Y., Song, C. C. and Zhang, J. B.: Dynamics of methane emissions from a freshwater marsh of northeast China, Sci. Total Environ., 371, 286-292, 2006.

Yrjala, K., Tuomivirta, T., Juottonen, H., Putkinen, A., Lappi, K. and Tuittila, E. S.: CH_4 production and oxidation processes in a boreal fen ecosystem after long-term water table drawdown, Glob. Change Biol., 17, 1311-1320, 2011.

Yu, K. W., Wang, Z. P., Vermoesen, A., Patrick Jr, W. H. and Cleemput, O. V.: Nitrous oxide and methane emissions from different soil suspensions: effect of soil redox status, Biol. Fert. Soils, 34, 25-30, 2001.

Yu, G., Lai, L. B. and Xu, B.: Preliminary Study on the responses of lake water from the western China to climate change in the future: Monte carlo analysis applied in GCM simulations and lake water changes, J. Lake Sci., 16, 193-202, 2004. (in Chinese with English abstract)

Zhang, J. B., Song, C. C., and Yang, W. Y.: Cold season CH4, CO2 and N2O fluxes from freshwater marshes in northeast China, Chemosphere, 59(11), 1703-1705, 2005.

Zhang, Y., Li, C., Trettin, C. C., Li, H., and Sun, G.: An integrated model of soil, hydrology, and vegetation for carbon dynamics in wetland ecosystems, Global Biogeochem. Cy., 16(4): 1061-1078, 2002.

Zhang, W., Yu, Y., Huang, Y., Li, T. and Wang, P.: Modeling methane emissions from irrigated cultivation in China from 1960 to 2050, Glob. Change Biol., 17, 3511–3523, 2011.

Zhang, X., Jiang, H., Lu, X., Cheng, M., Zhang, X., Li, X. and Zhang, L.: Estimate of methane release from temperate natural wetlands using ENVISAT/SCIAMACHY data in China, Atmos. Environ., 69, 191-197, 2013.

Zhuang, Q., Melillo, J., Kicklighter, D., Prinn, R. G., McGuire, A. D., Steudler, P. A., Felzer, B. S. and Hu, S.: Methane fluxes between terrestrial ecosystems and the atmosphere at northern high latitudes during the past century: A retrospective analysis with a process-based biogeochemistry model, Global Biogeochem. Cy., 18, GB3010, doi:10.102, 2004.

Zhuang, Q., Mellillo, J., Sarofim, M., Kicklighter, D. W., McGuire, A. D., Felzer, B. S., Sokolov, A., Prinn, R. G., Steudler, P. A. and Hu, S: CO_2 and CH_4 exchanges between land ecosystems and the atmosphere in northern high latitudes over the 21st century, Geophys. Res. Lett., 33, L17403, doi:10.1029/2006GL026972, 2006.

Zhuang, Q., Melillo, J., Mcguire, A., Kicklighter, D., Prinn, R. G., Steudler, P. A., Felzer, B. S. and Hu, S.: Net emissions of CH_4 and CO_2 in Alaska: Implications for the region's greenhouse gas budget, Ecolog. Appl., 17, 203-212, 2007.

Zhuang, Q., Chen, M., Xu, K., Tang, J., Saikawa, E., Lu, Y., Melillo, J. M., Prinn, R. G., and McGuire, A. D.: Response of global soil consumption of atmospheric methane to changes in atmospheric climate and Nitrogen deposition. Global Biogeochem. Cy., 27, 650-663, 2013.

Zhu, X. D., Zhuang, Q. L., Xiang, G., Sokolov, A. and Schlosser, C. A.: Pan-Arctic land-atmospheric fluxes of methane and Carbon dioxide in response to climate change over the 21st century, Environ. Res. Lett., 8, 045003, doi:10.1088/1748-9326/8/4/045003, 2013.

Table 1 Regional CH_4 emissions and the wetland area

		Region CH_4 emissions[$] (Tg)						Area[*] (M ha)					
		I	II	III	IV	V	China	I	II	III	IV	V	China
Inland Wetland	1950	2.80	0.31	0.25	0.06	0.11	3.53	12.26	4.78	2.66	0.30	0.27	20.27
	1980	2.06	0.27	0.22	0.06	0.10	2.71	9.71	4.61	2.57	0.29	0.26	17.44
	1990	1.90	0.23	0.14	0.09	0.08	2.44	7.73	3.42	1.77	0.44	0.18	13.54
	2000	1.13	0.23	0.13	0.05	0.07	1.61	5.40	3.43	1.41	0.23	0.15	10.62
	2010	1.16	0.22	0.12	0.05	0.06	1.61	5.09	3.20	1.36	0.20	0.13	9.98
	Decrease[#]	-58.6%	-29.0%	-50.40%	-16.7%	-45.5%	-54.4%	-58.2%	-33.3%	-48.1%	-33.3%	-66.7%	-50.8%
Coastal Wetland	1950	lt	nw	nw	0.09	0.18	0.27	lt	nw	nw	1.52	1.02	2.54
	1980	lt	nw	nw	0.08	0.09	0.17	lt	nw	nw	0.78	0.53	1.31
	1990	lt	nw	nw	0.05	0.07	0.12	lt	nw	nw	0.75	0.4	1.15
	2000	lt	nw	nw	0.05	0.06	0.11	lt	nw	nw	0.54	0.37	0.91
	2010	lt	nw	nw	0.06	0.04	0.10	lt	nw	nw	0.53	0.27	0.80
	Decrease[#]	lt	nw	nw	-33.3%	-77.8%	-62.9%	lt	nw	nw	-65.1%	-73.5%	-68.5%
Lakes and Rivers	1950	0.08	0.29	0.08	0.22	0.04	0.70	1.38	5.19	1.49	4.05	0.68	12.79
	1980	0.07	0.26	0.07	0.20	0.03	0.62	1.20	4.62	1.27	3.55	0.56	11.21
	1990	0.05	0.22	0.04	0.13	0.03	0.47	0.91	3.83	0.78	2.32	0.51	8.35
	2000	0.04	0.22	0.04	0.11	0.03	0.45	0.76	3.87	0.77	1.93	0.61	7.94
	2010	0.04	0.25	0.04	0.07	0.04	0.44	0.79	4.32	0.78	1.31	0.65	7.85
	Decrease[#]	-50.0%	-13.8%	-50.0%	-68.2%	0.0%	-37.1%	-42.8%	-16.8%	-47.7%	-67.7%	-4.4%	-38.6%
Total Wetland	1950	2.88	0.60	0.33	0.37	0.33	4.50	13.64	9.97	4.15	5.87	1.97	35.60
	1980	2.13	0.53	0.29	0.34	0.22	3.50	10.91	9.23	3.84	4.62	1.35	29.96
	1990	1.95	0.45	0.18	0.27	0.18	3.03	8.64	7.25	2.55	3.51	1.09	23.04
	2000	1.17	0.45	0.17	0.21	0.16	2.17	6.16	7.3	2.18	2.7	1.13	19.47
	2010	1.20	0.47	0.16	0.18	0.14	2.15	5.88	7.52	2.14	2.04	1.05	18.63
	Decrease[#]	-58.3%	-23.3%	-51.5%	-51.4%	-57.6%	-52.2%	-56.9%	-24.6%	-48.4%	-65.3%	-46.7%	-47.7%

[$] The average CH_4 fluxes of three consecutive years (including 1950—1952, 1979—1981, 1989—1991, 1999—2001 and 2008—2010) were used to calculated regional CH_4 emissions. For example, regional CH_4 emissions in 1980 were the production of the area of 1980 and the average CH_4 fluxes from 1979 to 1981.

[*] Data of 1980, 1990, 2000 and 2010 were from the remote sensing data (Niu et al., 2012). The area of 1978 and 2008 were regarded as the area of 1980 and 2010, respectively.

[#] Decrease means the reduce fraction in 2010 compared with 1950.

lt, less than 0.0001; nw, no wetland

Table 2 Estimation of CH_4 emissions from natural wetland in China.

Region	This study			Other studies			References
	CH_4 (Tg)	Period	Area (Mha)	CH_4 (Tg)	period	Area (Mha)	
China[$]	3.0	1990	23.0	2.2	1988－2000	Nm	Wang et al., 1993
China[$]	3.0	1990	23.0	1.7	1988	Nm	Khalil et al., 1993
China[$]	3.0	1990	23.0	2.0	1996	18.7	Jin et al., 1999
China[$]	3.0	1990	23.0	10.5	1990s	38.0	Wang et al., 2012
China[$]	3.0	1990	23.0	6.65	1990	35.5	Cai, 2012
China[$]	2.2	2000	19.5	5.71	2000	30.5	Cai, 2012
China[$]	2.2	2000	19.5	3.15	2000	Nm	Chen et al., 2013
China[$]	2.2	2000	19.5	4.76	2003－2009	9.0	Zhang et al., 2013
China[#]	3.5	1950	20.3	3.2	1950	17.9	Xu and Tian, 2012
China[#]	2.7	1980	17.4	2.3	1980	13.0	Xu and Tian, 2012
China[#]	2.4	1990	13.5	2.0	1990	11.0	Xu and Tian, 2012
China[#]	1.6	2000	10.6	1.9	2000	9.4	Xu and Tian, 2012
China[#]	1.6	2010	10.0	1.9	2008	9.4	Xu and Tian, 2012
China[#]	1.6	2000	10.6	1.9	1995－2004	9.4	Tian et al., 2011
China[#]	1.6	2000	10.6	1.8	1995－2004	9.4	Ding et al., 2007
NYC[#]	2.8	1950	12.3	2.2	1950	10.1	Xu and Tian, 2012
NYC[#]	1.2	2010	5.1	1.2	2008	4.7	Xu and Tian, 2012
NYC[#]	1.1	2000	5.4	1.2	2001－2002	2.8	Ding et al., 2004
NYC[#]	1.1	2000	5.4	0.9	2000	Nm	Chen et al., 2013
QHT[#]	0.3	1950	4.8	0.07	1950	0.8	Xu and Tian, 2012
QHT[#]	0.2	2008	3.2	0.06	2008	0.6	Xu and Tian, 2012
QHT[$]	0.45	1990	7.3	0.8	1996	3.5	Jin et al., 1999
QHT[#]	0.23	2000	3.4	0.56	2001－2002	4.8	Ding et al., 2004
QHT[#]	0.23	2000	3.4	1.25	2000	Nm	Chen et al., 2013

[$]Natural wetland

[#]Natural wetland exclude coastal wetland, lakes and rivers.

Nm, not mentioned in the literature

NYC, Northeast China

QTH, Qinghai Tibetan Plateau

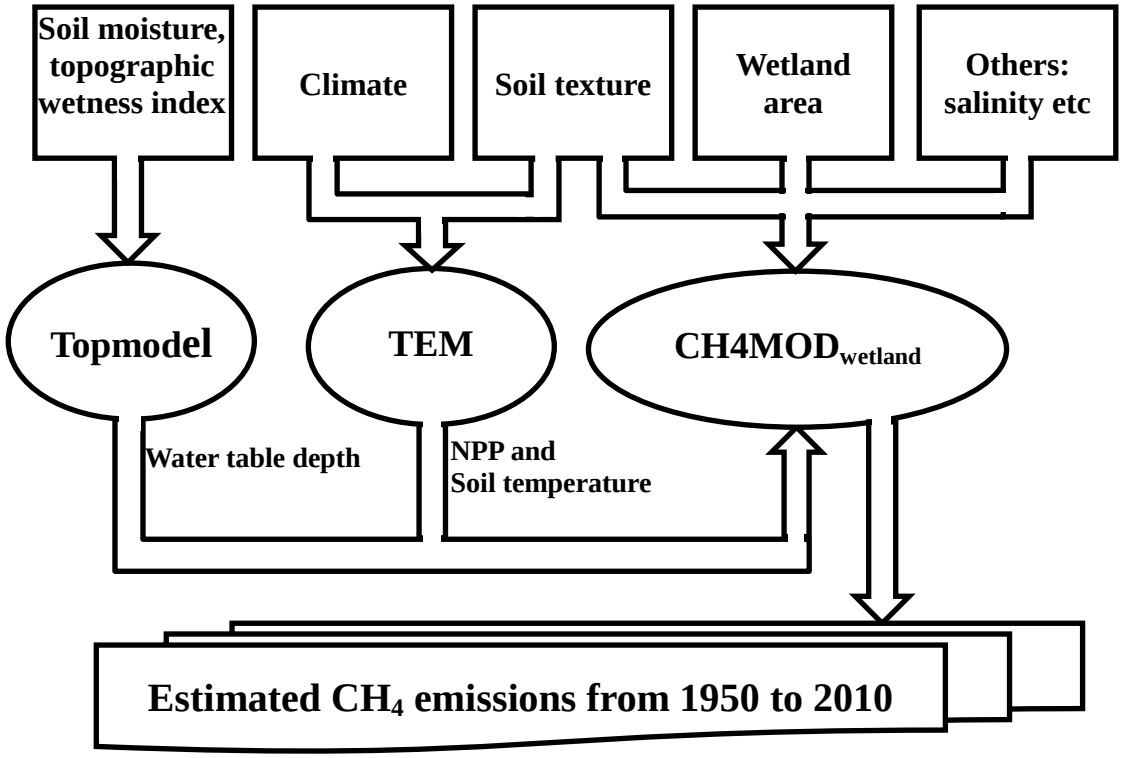

Fig. 1 Framework of simulating CH_4 emissions from natural wetlands between 1950 and 2010. CH4MOD$_{wetland}$ is a biogeophysical model to simulate CH_4 fluxes from natural wetlands. TEM is a process-based biogeochemistry model that couples carbon, nitrogen, water, and heat processes in terrestrial ecosystems to simulate ecosystem carbon and nitrogen dynamics. TOPMODEL is a conceptual rainfall-runoff model that is designed to work at the scale of large watersheds using the statistics of topography.

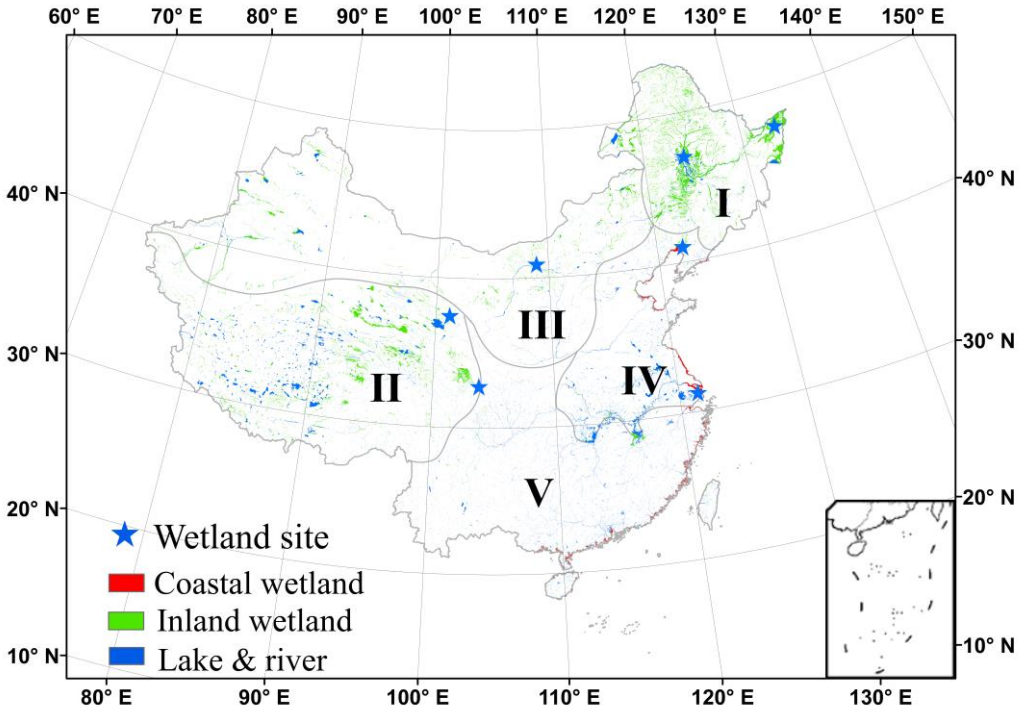

Fig. 2 Wetland regions across China. The blue stars are the locations of the wetland sites. The wetland distribution map is from the remote sensing data in 1978.

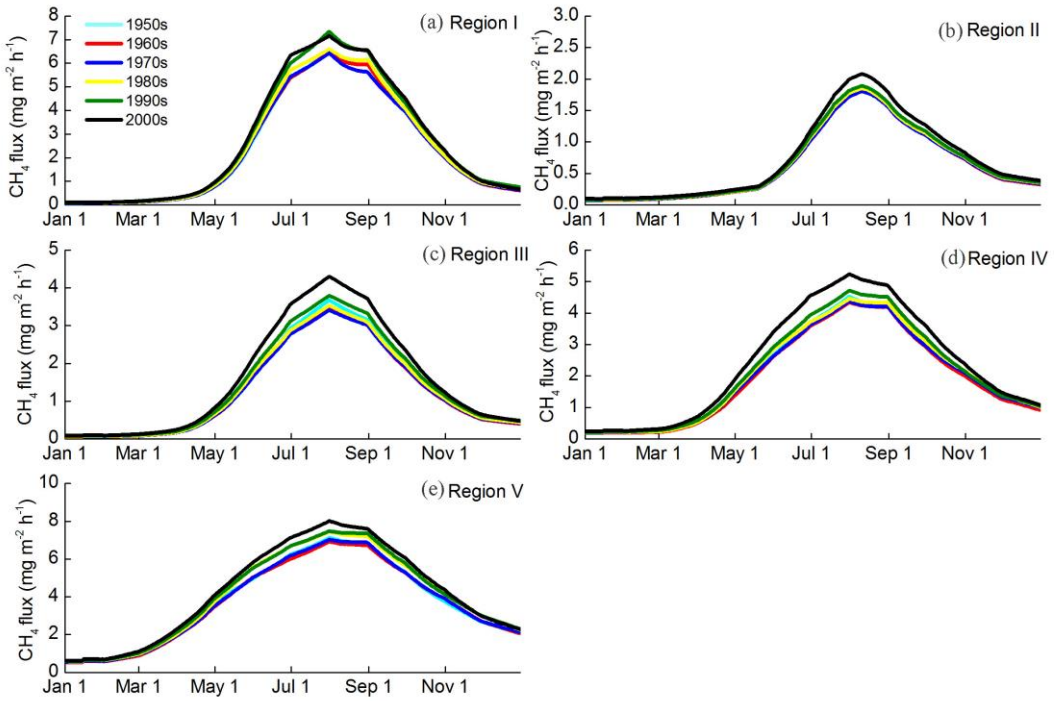

Fig. 3 Seasonal variations of methane fluxes in the five regions.

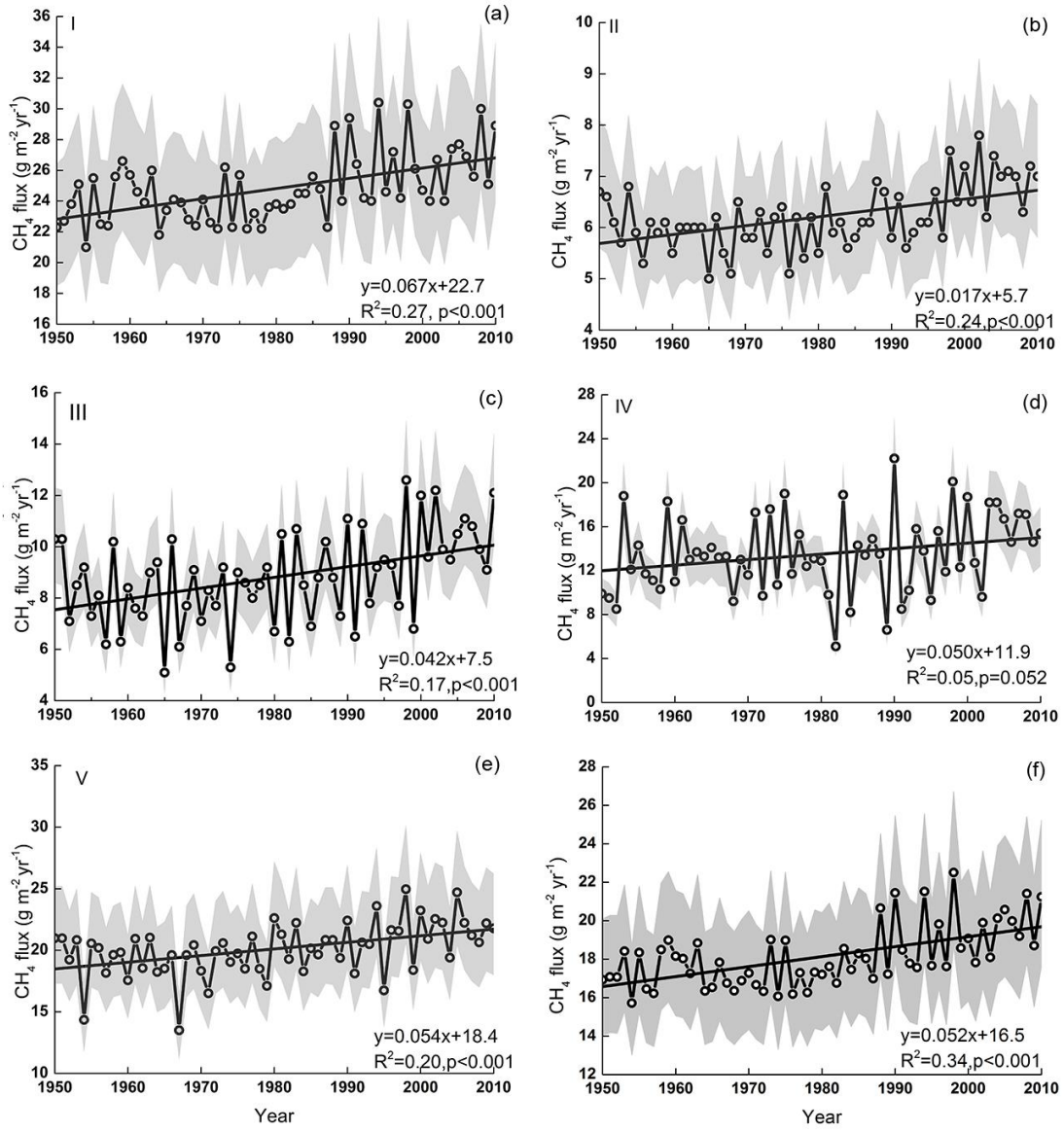

116

117 Fig. 4 Methane fluxes from inland and coastal wetlands between 1950 and 2010 in: (a)
118 Region I; (b) Region II; (c) Region III; (d) Region IV; (e) Region V. (f) China.

119

120

121

122

123

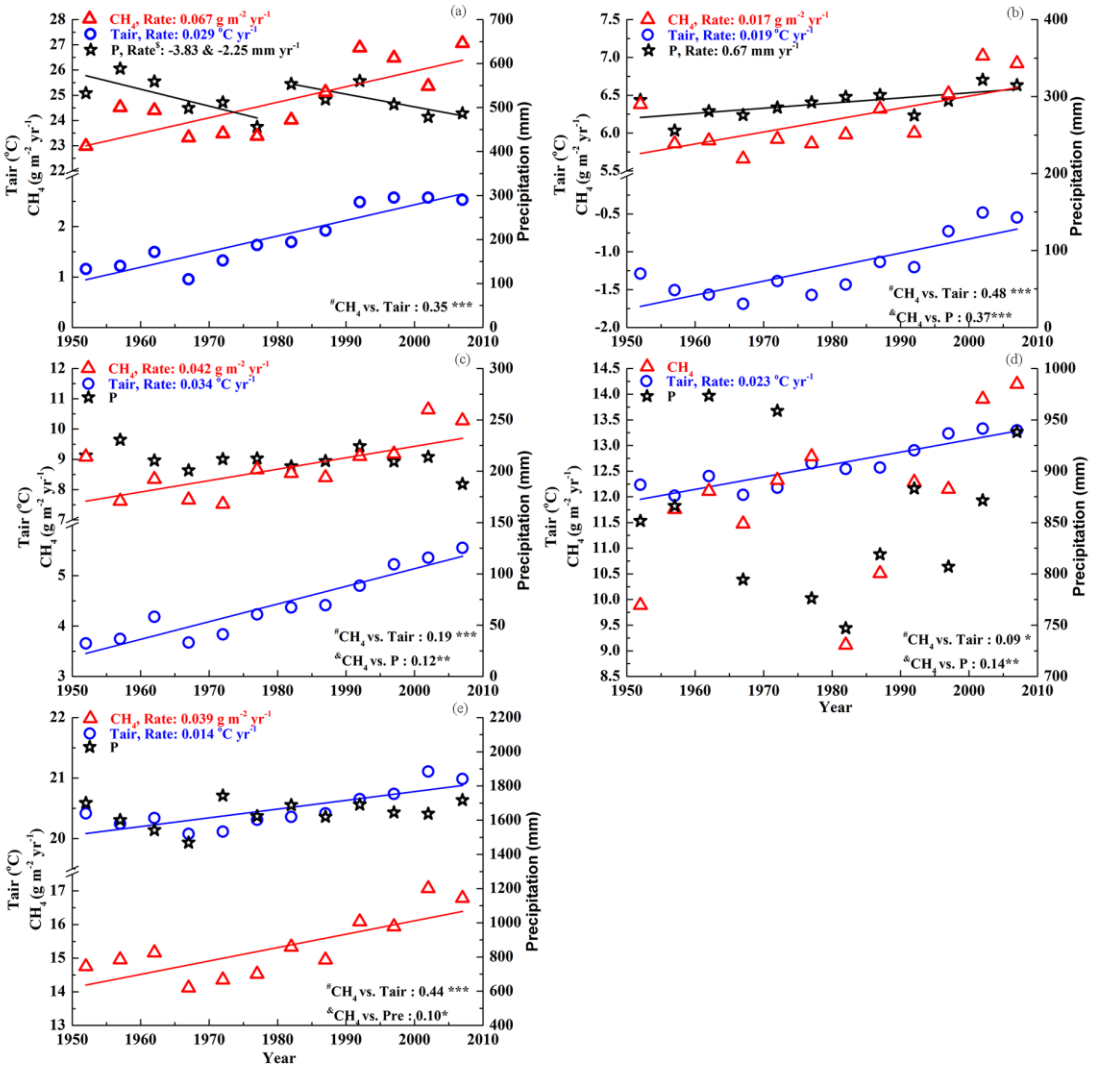

Fig. 5 Impact of the climate factors on CH_4 fluxes from 1950 to 2010 in: (a) Region I; (b) Region II; (c) Region III; (d) Region IV; and (e) Region V. The red triangles, blue circles and the black stars are 5-year average CH_4 fluxes (the same data as in Fig. 4), air temperature and precipitation, respectively. The slope represents the significant linear rate ($p<0.05$). CH_4 vs. Tair: the correlation coefficient between the annual mean CH_4 fluxes and air temperature. CH_4 vs. P: the correlation coefficient between the annual mean CH_4 fluxes and the precipitation. Only correlations with statistical significance are shown ($p<0.05$).